Electrophysiological investigations of retinal and polarization sensitivity in rainbow trout (*Oncorhynchus mykiss)*

By

Leslie Gayle Anderson
B.A., University of Alberta, 1983
M.P.A., University of Victoria, 1989
B.Sc., University of Victoria, 2002

A Thesis Submitted in Partial Fulfillment of the Requirements for the Degree of

Master of Science

In the Department of Biology

Electrophysiological investigations of retinal and polarization sensitivity in rainbow trout (*Oncorhynchus mykiss)*

By

Leslie Gayle Anderson

B.A., University of Alberta, 1983

M.P.A. University of Victoria, 1989

B.Sc., University of Victoria, 2002

Supervisory Committee

Dr. Craig Hawryshyn
Supervisor

Dr. Dorothy Paul
Departmental Member

Dr. Paul Zehr
Outside Member

Dr. David Docherty
External Examiner

Supervisory Committee

Dr. Craig Hawryshyn
Supervisor

Dr. Dorothy Paul
Departmental Member

Dr. Paul Zehr
Outside Member

Dr. David Docherty
External Examiner

Abstract

Understanding how animals detect and discriminate different qualities of light is a key component of the study of visual ecology. My research investigated the use of three electrophysiological methods to assess the neuronal mechanisms involved in spectral and polarization sensitivity in one species of salmonid, the rainbow trout (*Onchorynchus mykiss*). I examined the neuronal mechanisms underlying polarization sensitivity using electroretinograms (ERG) and optic nerve compound action potential (CAP) recordings. Chromatic adaptation and pharmacological techniques were used to reveal opponent interaction at the cone-horizontal cell level and to provide the first evidence of retinal processing of polarization sensitivity. To facilitate additional research more suited to the exploration of neural networks and signaling, I developed the protocols and techniques necessary to investigate the spectral sensitivity of rainbow trout using whole-cell patch clamp (WPC) electrophysiology, and produced the first assessment of the ultraviolet component of spectral sensitivity in a vertebrate using this technique.

Table of Contents

List of Tables

List of Figures

Acknowledgements

As my sister pointed out partway through this endeavour, if you already knew where the path was going, you wouldn't really learn anything by pursuing it. The research described in the pages that follow can certainly, therefore, be considered part of a true learning experience and I feel genuine gratitude for those who helped me maintain momentum and some semblance of sanity along the way.

Thanks go first to Dr. Craig Hawryshyn for keeping the journey interesting and for tolerating my persistent wanderings into the more philosophical questions raised by our work. I would also like to express my wholehearted appreciation to my lab mates, including Dr. William (Ted) Allison, Dr. Shelby Temple, and Martina Mussi for their camaraderie, constructive suggestions, and exemplary perseverance. I would like to particularly thank Sam Ramsden who, in addition to the qualities described above, brought a high degree of professionalism and humour to all of our work together and helped make many dark hours in the hut pass more pleasantly and fruitfully. Theo Haimberger deserves special acknowledgement for his continuous efforts to connect the theory and reality of the equipment and knowledge I needed to carry out this research.

I owe an indescribable debt to Dr. James Plant for his tireless encouragement and support. Gaining 'Renaissance-man Jim' as a friend is undoubtedly the bonus prize for undertaking this program. Thank you Jim, for sharing your knowledge of patch-clamping rituals, your enthusiasm for exploration, and for choosing the paths you believe in.

Dr. Maarten Kamermans and members of his lab in Amsterdam, particularly Dr. Iris Fahrenfort, also deserve thanks for taking the time to provide hands on patch-clamp training, without which I would have been on this journey without a paddle.

My Committee members also merit recognition for their patience and leadership. In particular Dr. Dorothy Paul was always available to discuss my research and both encouraged and guided my neuroscience musings, whether rooted in questions of ions, behaviour, ethics or the whole host of connections in between. In addition, several members of the department are known among the grad students as having a genuine interest in supporting student research, and I would like to acknowledge Drs. Louise Page, Nancy Sherwood, Francis Choy and Brad Anholt for taking the time to ask, listen, and offer words of support and advice.

Throughout my life I've been fortunate to be surrounded by family that has consistently encouraged the pursuit of the intriguing. Over the past few years, they have shown remarkable dexterity in maintaining support for my pursuits while balancing all other aspects of our lives. Thanks go especially to my partner Kim for being committed to adventure and to Elise and Danielle for waiting, most of the time, for those moments when I said they could help mommy on her computer. Special gratitude goes to my sister Laura, for maintaining her tradition of unrelenting interest, honesty and cortex-cutting humour. Without your insights I would feel very differently about this work and its place in my life. My appreciation for the mysteries of vision, spirit and life would be entirely different and less rich without you.

And finally, to my mother, who passed the parenthood baton as I was beginning this academic journey, my appreciation and respect for what you've given me grows each day, and I hope I can do justice to the faith you put in me. I miss you like crazy.

List of abbreviations

CNS	Central nervous system
ERG	Electroretinogram
GABA	Gamma-aminobutyric acid
HBW	Half band width
HC	Horizontal cell
I	Current
INL	Inner nuclear layer
IPL	Inner plexiform layer
LWS	Long wavelength sensitive
MSP	Microspectrophotometry
MWS	Medium wavelength sensitive
nm	nanometers, 10^{-9} meters
ONL	Outer nuclear layer
OPL	Outer plexiform layer
PS	Polarization sensitivity
SWS	Short wavelength sensitive
UV	Ultraviolet
UVS	Ultraviolet sensitive
V	Voltage
WPC	Whole-cell patch clamp
λ_{max}	Lambda max; the spectral position of the main peak of the absorbance spectrum of a visual pigment

Chapter 1: Thesis Introduction

Color and all vision are in a sense illusory depending only on messages that pass between millions of neurons that reside within the darkness of our skull. These visual messages allow us to project ourselves into a universe that would be unknown to us without vision (Gouras, 2006).

Almost all living organisms, plant and animal, are sensitive to light. Humans rely extensively on the sense of sight to establish, perceive and navigate the external world. In general, we expect our eyes to be reliable and comprehensive transmitters of the world around us. Research investigating visual experiences occurring outside or beyond our sensory capabilities is a fascinating reminder that there is more going on in the universe than meets the human eye.

Since at least the days of von Frisch's (1949) insightful investigation into the navigational capacities of bees using polarized light, there has been increasing evidence that many species perceive the electromagnetic spectrum in ways unavailable to human senses. The research described in this thesis contributes to the assessment of the roles of individual retinal cell types in processing two such visual cues – ultraviolet and polarization stimuli. In this introduction I will provide:

- a brief outline of photoreception and the evolution of the study of spectral and polarization sensitivity in the field of visual ecology;
- a description of the neural anatomy of the retina – the structure that is responsible for the initial detection and coding of visual signals; and
- a summary of the role of the retinal neural network (in particular horizontal cells) in shaping neural coding of spectral and polarization stimuli.

An Overview of Visual Photoreception

The stimulus for vision is visible light, a small band of energy contained within the electromagnetic spectrum. The electromagnetic spectrum forms a continuum from very

longwave and low-energy radio waves, with wavelengths as long as 10^{+4} meters, to shortwave high-energy gamma rays with wavelengths as short as 10^{-12} meters. Only a very small portion of this spectrum with wavelengths on the order of 10^{-6} meters is visible to animals as light. Radiation below 320 nm, ultraviolet A (UVA), is largely screened out by the ozone layer in the Earth's upper atmosphere and is therefore unavailable to the visual system, but radiation above 320 and below 400 nm (UVB) can be perceived by an extensive variety of animal species – many of which possess photoreceptor cells maximally sensitive in this range. In some species, however, including humans, absorbance by the lens in the shorter-wavelength region truncates sensitivity at around 400 nm (Thorpe et al., 1993).

The visual process begins[1] when visible light enters the eye and stimulates cells in the retina. The retina includes both sensory neurons that respond to light (the photoreceptors) and intricate neural circuits that perform the first stages of image processing. Much of the construction of an image takes place in the retina itself through the use of these specialized neural circuits. Ultimately, an electrical message travels down the optic nerve into the brain for further processing and visual perception.

In vertebrates, sensitivity to light is achieved by the presence of rod and cone photoreceptors in the retina. Normally, rods are active at low (scotopic) light intensities, and cones at high (photopic) intensities. Photoreceptors are composed of an inner and an outer segment, nucleus and synapse. Light sensitivity is conferred by visual pigment molecules embedded in the disc membranes of the outer segment; each type or class of photoreceptor contains a visual pigment differing from others in its peak of spectral sensitivity (λ_{max}). The visual pigment molecules are G-protein-coupled receptors

[1] if we ignore for the sake of simplicity, but not necessarily accuracy, the signals from the brain to the retina which guide and shape what is seen.

composed of a protein (opsin) and a chromophore (an aldehyde of either vitamin A1 or A2). The visual pigment's spectral sensitivity depends both upon the chromophore and the opsin, but for a given chromophore the shape of the curve is a predictable function of the peak wavelength (Dartnall, 1953; Govardovskii *et al.*, 2000). Usually a single photoreceptor cell contains one type of visual pigment, but there are exceptions, the best known being the presence of mixtures of A1 and A2 visual pigments in fish and amphibians (see Reuter et al., 1971; Wald 1939, 1946; chapter 2). Visual pigments convert information on light intensity and spectral composition; neural processing can then extract further information such as frequency of stimulus, contrast, movement, and polarization information. Four main gene families of vertebrate cone opsin have been recognized (Bowmaker & Hunt, 1999; Hisatomi *et al.*, 1994), distinguished on the basis of the amino acid sequence of their respective opsins, and they roughly correlate with spectral sensitivity: long-wavelength sensitive (LWS) with λ_{max} 500–570 nm, middle-wavelength sensitive (MWS) with λ_{max} 480–520 nm, short-wavelength sensitive (SWS) with λ_{max} 415–470 nm, and violet/ultraviolet sensitive (VS/UVS) with λ_{max} lying between 355-435 nm. The presence of two or more different cone classes each with a different λ_{max} enables the visual system to sample light levels at different spectral locations. However, the presence of differentially sensitive photoreceptors alone is not sufficient for colour vision. The discrimination of colour requires the presence of a neural opponency system to compare the photon catch by different cone photoreceptors.

The Study of Spectral and Polarization Sensitivity

As the study of human colour vision and psychophysics became established in the 19th century, researchers also began investigating whether other species see colour. Lubbock (1888) in his book *On the Senses, Instincts and Intelligence of Animals* developed behavioural criteria to demonstrate that *Daphnia* sp. see colour, using the fact that they are both positively phototactic and prefer yellow to white light, which is more intense across the entire spectrum. Concepts in colour vision are mostly derived from human perception and psychophysics. Most mammals have two classes of cone visual pigments, although humans possess three. Human trichromacy was first proposed early in the nineteenth century (Young, 1802), and models relating our colour discrimination to underlying receptor responses and neural mechanisms are well over a century old (Helmholtz, 1896; Hering, 1878; Maxwell, 1860). The initial focus of studies that went beyond a behavioural demonstration of the existence of colour vision and began to investigate receptor inputs and neural mechanisms was on mammals (see Jacobs, 1981), although important work was also performed with honeybees (Daumer, 1956; von Helversen, 1972).

More recently, fish have been used extensively in the study of mechanisms of signal processing in the retina. Fish inhabit a tremendously diverse range of habitats and as a result have developed a similarly wide range of visual adaptations. Over the last 25 years, research investigating colour vision in fishes has been widespread (e.g. see Bowmaker, 1995; Levine and MacNichol, 1982; Lythgoe, 1988). Following the identification of an ultraviolet (UV) absorbing visual pigment in the dace, a species of cyprind fish, (Harosi & Hashimoto, 1983) research has begun to accumulate demonstrating that UV sensitivity is widespread in fishes (Avery et al., 1983; Bowmaker, 1998; Hawryshyn and Beauchamp, 1982, 1985; Neumeyer, 1992; reviewed in Douglas et al., 1989 and Losey et al., 1999) as well as other vertebrates (e.g.,

Bennet & Cuttill, 1994; Burkhhardt, 1989; Jacobs, 1992; Tovee, 1995). However, in spite of the knowledge that four classes of cone visual pigments are present in many vertebrate classes, visual neuroscience research is still often conducted in the context of trichromacy. Studies and reviews concerning the detection and processing of different wavelengths of light, and related behaviours in species with known UV sensitivity still frequently do not include an assessment of the ultraviolet contribution (e.g., Kraaij et al., 1998; Pang et al., 2002; Piccolino, 1995; Wietsma et al., 1995; Yamada et al., 1992). In part this may be attributed to the challenges associated with designing equipment and protocols appropriate for working in the range below 400nm, but it may also be the result of a human tendency to overlook stimuli that escape our own sensory abilities.

In fishes UV-sensitivity is proposed to enhance the detection of zooplankton (Bowmaker and Kunz, 1987; Browman and Hawryshyn, 1994; Loew et al., 1993) and to play a role in conspecific recognition (Harosi, 1985; Loew and McFarland, 1990), and its functionality extends beyond colour discrimination. Coughlin and Hawryshyn (1994a) demonstrated that UV stimuli appear to be processed primarily in the torus semicircularis, an area that also receives input from acoustic, lateral line and electrosensory systems (Schellart and Rikkert, 1989), as opposed to the optic tectum, which is considered the primary visual area (Meek, 1990) responsible for a suite of visual stimuli processing functions – including determining velocity and direction of movement, detection of borders and patterns, and wavelength discrimination (Guthrie, 1990). In addition, an important link exists between the presence of ultraviolet sensitivity and polarization sensitivity, as functional polarization vision appears to operate only in the UV part of the spectrum (Hawryshyn, 2000).

The linear polarization of light is a function of the characteristics of electromagnetic radiation and the earth's atmosphere. Light is a wave of electromagnetic energy made up of an electric field and a magnetic field that oscillate at right angles to

each other. The orientation of the electric field is described by a vector (referred to as the 'e-vector') that is perpendicular to the direction in which the wave is traveling (Figure 1.1). Although the sun emits light in all directions, the light that is scattered to earth from the atmosphere is said to be "polarized" because only certain orientations of e-vector reach the earth's surface (i.e., those aligned in such a way to as to pass through the atmosphere without being redirected out to space).

Many species of fish have evolved visual mechanisms for the perception of linearly polarized light and behaviours based on this perception (Hawryshyn and McFarland, 1987; Hawryshyn et al., 2003; Mussi et al., 2005; Parkyn and Hawryshyn, 2000; Parkyn et al., 2003; Shashar et al., 1996; 1998; Shashar and Hanlon, 1997; Waterman and Hashimoto, 1974). In both salmonids and cyprinids, the UV-sensitive cone mechanisms exhibit maximum polarization sensitivity to a vertically oriented e-vector, while the mid-wavelength-sensitive and long-wavelength sensitive cone mechanisms show maximum sensitivity to a horizontally oriented e-vector (Hawryshyn and McFarland, 1987, Parkyn and Hawryshyn 1993, 2000). Neuronal coding of e-vector therefore appears to occur as a result of differential responses in UV-sensitive cones. As is the case with colour vision, polarization vision requires a neural network that processes polarization input from the photoreceptors and would involve the neural processing of, and interaction between, the channels transmitting differential polarization sensitivity.

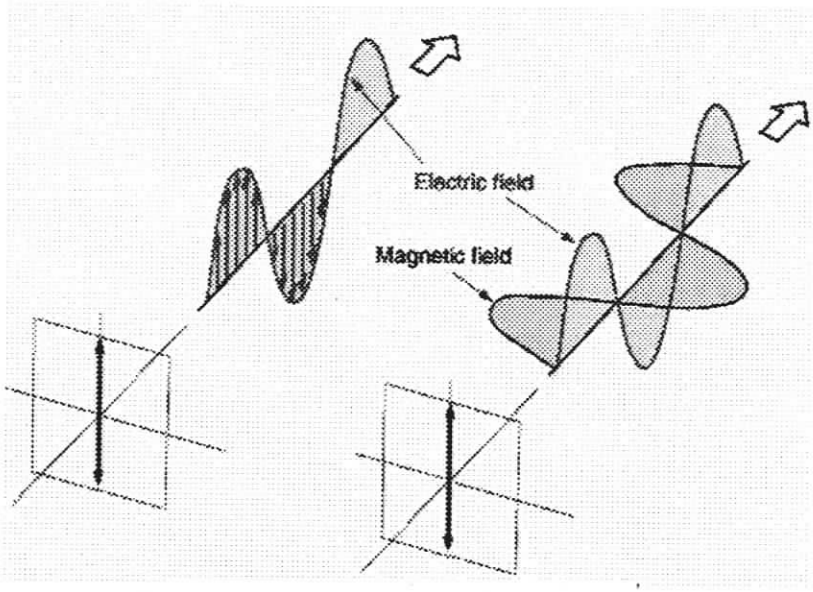

Figure 1.1 A plane electromagnetic wave is said to be linearly polarized. The transverse electric field wave is accompanied by a magnetic field wave as illustrated (from Nave, 2006).

Retinal neuro-anatomy and the role of photoreceptors and horizontal cells in shaping UV- and polarization-sensitivity

The retina of teleost fish is a layered neuronal structure, about a quarter of a millimeter thick, in which at least seven different cell types can be distinguished (Figure 1.2). The output synapse of rod and cone photoreceptors is the crucial link between the transduction of light and the neural processing of that signal. At this first synapse there is communication not only from the photoreceptors to second order bipolar and horizontal cells, but both inhibitory and excitatory feedback communication from these second order cells to photoreceptors.

Retinal horizontal cells, together with bipolar cells, are the first neurons to receive light information from the photoreceptors. The 'through' pathway for light signals in the retina is from photoreceptors to bipolar cells to ganglion cells, which form the optic nerve. In general, horizontal cells receive synaptic input from photoreceptors and transmit lateral inhibitory signals within the outer plexiform layer to other photoreceptors and/or bipolar cells (Yazulla, 1995). Horizontal cells that contact cone photoreceptors in teleosts are divided into two main types: luminosity (L-type) that hyperpolarize to all spectral stimuli, and chromaticity (C-type) that hyperpolarize in response to some wavelengths and depolarize in response to others (Wagner, 1990). Horizontal cell feedback has been shown to be involved in retinal mechanisms analyzing temporal, spatial, and chromatic features of the visual signal, as well as neural control of light sensitivity (Fuortes *et al.*, 1974; O'Bryan, 1973; Pasino and Marchiafava, 1976; Werblin, 1974). In particular, this feedback pathway is thought to form the basis of the colour-opponent responses in C-type horizontal cells when photoreceptors are stimulated by different wavelengths of light (Fuortes and Simon, 1974; Kamermans *et al.*, 1991; Stell and Lightfoot, 1975) and of the surround responses of bipolar cells (Kaneko, 1970;

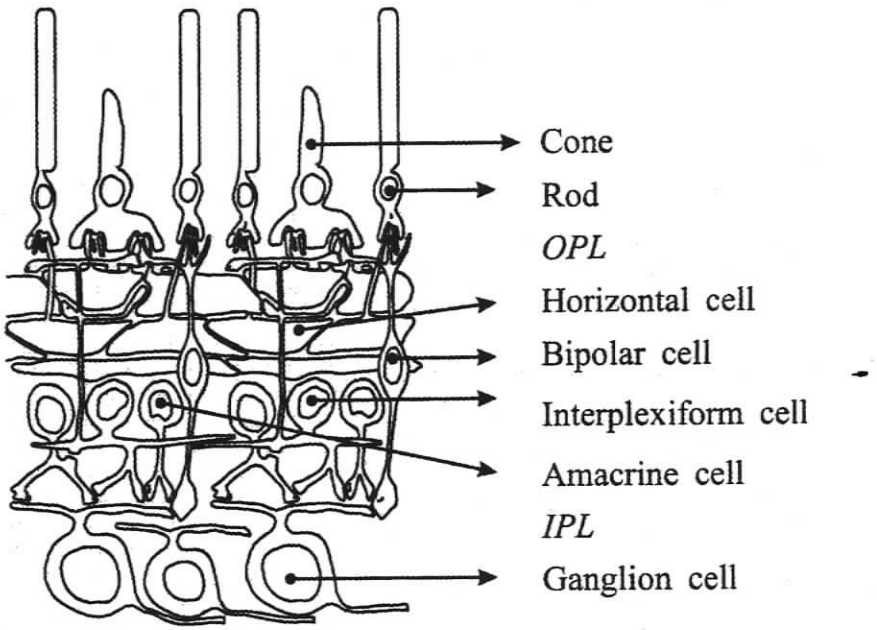

Figure 1.2: Schematic cross-section of the retina (from Dowling and Ehinger, 1978).
Define OPL and IPL

Kaneko, 1973). More recently, they have been considered a part of a feedback system to produce colour constancy (Kamermans *et al.*, 1998).

It is possible that horizontal cells play a significant role in processing both ultraviolet and polarization sensitivity, and different classes of horizontal cells may exist to mediate the horizontal and vertical channel inputs from MWS/LWS and UVS cones respectively. However, to date there has been no characterization of the processing of polarization sensitivity within the retina.

Scope and Aims of Thesis

The objective of my research was to investigate the role of photoreceptors and horizontal cells in processing ultraviolet and polarization stimuli. Working with rainbow trout, *Onchorynchus mykiss*, a species with known UV and polarization sensitivity (Hawryshyn and Harosi (1994); Parkyn et al. 2000), I developed protocols and conducted experiments to:

- Assess the spectral sensitivity of cone photoreceptors using whole-cell patch clamp technique (Chapter 2), and
- Investigate the influence of horizontal cell signaling on polarization and spectral sensitivity using electroretinograms (ERGs) and pharmacology (Chapter 3).

Chapter 2: Spectral sensitivity of the cones in rainbow trout (*Oncorhynchus mykiss)* determined using patch clamp electrophysiology

This chapter is based on a collaboration with the following authors and is in preparation as cited below:

L.G. Anderson, T.J. Haimberger, and C.W. Hawryshyn (in prep). Spectral sensitivity of the cones in rainbow trout (*Oncorhynchus mykiss*) determined using patch clamp electrophysiology.

Introduction

One of the primary model systems for studying cell signaling is based on transduction in vertebrate photoreceptors and the related neural pathways and processing of vision. Since initial reports of a 'new' type of cone photoreceptor containing an ultraviolet (UV) absorbing visual pigment in three species of cyprinid fish (Avery *et al.,* 1983; Harosi and Hashimoto, 1983; Harosi, 1985), research demonstrating an increasing number of vertebrate species with visual sensitivity to UV light has been presented (see Jacobs, 1992 for review). Investigations into the transduction and neural processing of UV signals are, however, remarkably few, in part as a result of the challenges in terms of both technique and equipment (see Losey *et al.,* 1999 for review).

The visual system of rainbow trout as well as of other Pacific salmonids is currently of interest to those studying UV photoreception and its functional implications, including sensitivity to UV-polarized light (Hawryshyn 1992, 2000). Examination of sensitivity to UV light in salmonids has incorporated psychophysical techniques (Hawryshyn *et al.,* 1989), microspectrophotometry (Hawryshyn and Harosi, 1994, Hawryshyn *et al.,* 2001; Temple, 2006), compound action potential recordings (Beaudet *et al.*, 1993; Coughlin and Hawryshyn, 1994b; Deutchlander *et al.,* 2001; Parkyn and Hawryshyn, 2000; and more recently, molecular work (Veldhoen *et al.*, 2006; Dann *et al.*, 2003) and electroretinograms (Allison *et al.,* 2003). Hawryshyn (2000) hypothesized that interneuronal processing, specifically interaction between the contributions of the UVS and LWS mechanisms facilitated by horizontal cells, could be responsible for the coding of e-vector. Further development of a model examining the neuronal processing and encoding of UV and polarization stimuli requires the development of protocols in which photoreceptors retain their cellular connections and the underlying currents in cell signaling can be characterized.

The whole-cell patch-clamp technique has emerged as a powerful tool in the characterization of cellular behaviour and, when applied to cells in a neural network that are alive and intact, can be used in the elucidation of intercellular signaling. However, few studies have used the patch clamp recording technique to assess spectral sensitivity or photocurrent activity. The whole-cell patch-clamp has recently been used to assess the photoreceptor responses in an invertebrate (cuttlefish, *Sepia officinalis,* Chrachri *et al.*, 2005) and the spectral sensitivity of three of the four cone classes in the goldfish (Kamermans *et al.*, 2001; Kraaij *et al.*, 1998; 2000a and b, Verweij, 1996). Suction pipette electrodes have been used to measure membrane photocurrents of cone photoreceptors in two cyprinids (goldfish, *Carassius auratus,* Palacios *et al.*, 1998; and the giant danio, *Danio aequipinnatus,* Palacios *et al.*, 1996) as well as in the monkey (Baylor *et al.*, 1987). To date, only the work by Palacios *et al.*, (1996, 1998) has included an assessment of UV-sensitivity.

In order to facilitate further development of models of neural processing of ultraviolet photosensitivity, I undertook the development of protocols and techniques to examine current responses in individual cone photoreceptors to light stimuli using whole-cell patch clamp electrophysiology in an isolated retina preparation.

Materials and Methods

Animals

Juvenile rainbow trout (*Oncorhynchus mykiss*) between 3 -10 g body mass were obtained from the Fraser Valley Trout Hatchery, Abbottsford, B.C., Canada. Fish were held on a 12hr:12hr light:dark photoperiod and maintained at 15+/-1°C. The photic conditions within the holding facility were provided by full spectrum florescent bulbs. All

experimental procedures and care were approved by the University of Victoria Animal Care Committee under the auspices of the Canadian Council for Animal Care.

Preparation of the tissue

Rainbow trout were kept in the dark for 8 ± 1 minutes to facilitate the isolation of the retina from the pigment epithelium while keeping the retina light adapted. Fish were anesthetized in a solution of 250 mg l^{-1} tricane methanesulphonate (MS-222) during the last 2 minutes of this dark phase and then euthanized by cervical transaction. Under dim red light, an eye was enucleated, hemisected and most of the vitreous was removed with filter paper. In some cases, both eyes were removed and one eye was used immediately while the other was maintained in darkness at 4°C in oxygenated Ringer's solution for 2-3 hours before recording. The retina was isolated, placed photoreceptor side up in a superfusion chamber and superfused continuously (1.5ml min^{-1}) with oxygenated Ringer's solution (pH 7.7, 17°C).

The superfusion chamber was mounted on a Nikon Eclipse 600FN microscope (Nikon, Canada). The preparation was illuminated with infrared light (λ > 850nm) and viewed with a Nikon 60X water immersion objective, Nomarski optics for contrast modulation, and a video CCD camera (Canadian Photonic Laboratory, Minnedosa, Manitoba).

Optical system

A 150W xenon lamp and monochromator (Photon Technology International (Canada), London, Ontario) were used to supply narrow band stimuli (10 nm half bandwidth). Duration of flash was controlled by an electronic shutter (Uniblitz, Vincent

Associates, Rochester, NY), and intensity was controlled by an Inconel quartz neutral density filters. Sixty-µm spots were projected through the 60x immersion objective of the microscope.

Electrodes and solutions

Electrodes were pulled from glass capillaries (Schott #8250, 1.5/1.0 (OD/ID mm)) (WPI, Sarasota Florida) with a Sutter P-97 micropipette puller (Sutter Instruments Company, Novato, CA) and had impedances between 6-9 MOhm when filled with pipette medium and measured in Ringer's solution. Electrodes were mounted on a three-axis piezio-electric EXFO micromanipulator (Burleigh, Concord, Ontario) and connected to an Axon Multiclamp 700A amplifier (Molecular Devices, Sunnyvale, CA).

The Ringer's solution contained (in mM) 102.0 NaCl, 2.6 KCl, 1.0 $CaCl_2$, 1.0 $MgCl_2$, 28.0 $NaHCO_3$, 5.0 glucose and was continuously bubbled with approximately 2.5% CO2 and 97.5% O2 yielding a pH of 7.8. The pipette medium contained (in mM) 11.7 KCl, 60.0 KGlu, 1.0 $MgCl_2$, 0.1 $CaCl_2$, 5.0 EGTA, 5.0 HEPES, 3.9 ATP_{Na}, 0.1 GTP_{Na}, 0.2 $cGMP_{NA}$, 20.0 Phosphocreatine, and 0.6 Creatine phosphokinase. The pH of the pipette solution was adjusted to 7.25 with KOH. Chemicals were obtained from Sigma-Aldrich (Oakville, Ontario).

Recording procedure

Individual photoreceptors were visually identified in the eyecup preparation and recordings were obtained by lowering a patch electrode directly onto the cell while monitoring current response to 5 mV voltage pulses and then applying suction to the cell to produce a > 1 GOhm seal.

To measure photocurrents, whole-cell recordings were made under voltage clamped (V= -60 mV) conditions, while the retina was stimulated with 100ms flashes of various wavelengths and intensities. Stimulus size was a 60 μm spot, and the interstimulus interval was always more than 5000ms. The stimulus and recording protocol was derived from previous whole-cell electrophysiology studies of spectral sensitivity in other species of fishes (Kraaij *et al.*, 1998; Palacios *et al.*, 1998) and on experiments I conducted to assess the impact of the total photon load per μm^2 delivered over the duration of the stimulus on tissue viability and cell response.

Sampling of wavelengths followed a protocol based on the visual identification of cell type as being either a single or double cone member, in each case testing several wavelengths near the expected lambda max values and then randomly between 300 and 680nm for double cones, and between 300 and 520nm for single cones. For the series of measures taken for each wavelength, the maximal photocurrent response (p) between 100 and 400ms after light onset was divided by the maximal current response for the series (p_{max}) and plotted against the stimulus intensity. A Naka-Rushton (Naka and Rushton, 1966) function (Equation 1) was fitted to the resulting response versus intensity curves and a criterion chosen that intersected with the linear dynamic range of these curves. These threshold responses were used to produce threshold versus intensity curves, and the inverse of threshold intensity was defined as sensitivity to the wavelength.

$$p(\lambda, I) = p_{max} \frac{I^n}{S(\lambda)^n + I^n} \qquad (1)$$

Where $p(\lambda, I)$ is the sustained response amplitude of the cone (in pA), p_{max} is the maximal sustained response amplitude of the cone (in pA), I is the stimulus intensity (in

photons μm^{-2} s^{-1}), S (λ) is the intensity needed for a half-maximal response (in photons μm^{-2} s^{-1}), *n* is the slope factor, and λ is the stimulus wavelength (in nm).

Analysis of kinetics and flash sensitivity

For the analysis of kinetics and flash sensitivity, four to seven representative cells were selected from each cone and individual responses to flash stimuli were smoothed using a 79-point box-car smoothing function. For several wavelengths near the lambda max for each cell, two to four individual responses to flash stimuli were averaged to calculate the peak amplitude and time to peak for each cell. These results were combined to establish averages for each cone type. Sensitivity to 100 ms flash stimuli at selected wavelengths was defined as the peak response (pA) /Intensity (in photons $flash^{-1}$ μm^{-2}) (Palacios & Goldsmith, 1993). Comparison among the mean time-to-peak and sensitivity of the cone types was made using a one way analysis of variance (ANOVA) with α=0.05.

Analysis of spectral sensitivity data/assignment of Lambda max (λ_{max})

Data consisting of values of log sensitivity at a number of discrete wavelengths were collected for each cell. The wavelength of peak sensitivity, or lambda max (λ_{max}), was estimated for each cell by fitting a template (Govardovskii *et al.*, 2000) by eye to the sensitivity plot generated by the threshold versus intensity curves. The individual values of λ_{max} obtained for each cell were averaged to characterize the population.

The amplitude of cell responses is affected by various patch characteristics, with the quality of the seal between the cell membrane and the electrode being a significant

factor, resulting in spectral sensitivity data from different cells being displaced vertically on the sensitivity axis. To address this between-cell variation in apparent sensitivity, data for each cell were normalized by setting the wavelength of maximum response as = 1 and wavelength of minimum response = 0. Data from cells within individual cone types were then combined to obtain average values of normalized sensitivity (NS) for each wavelength. In addition, the consistency of responses across cell types was examined by comparison of responses against a normalized frequency template. Relative spectral sensitivity (RS) was defined for each cell as the lateral shift of the various wavelength curves at half-maximal response amplitudes relative to the most sensitive stimulus wavelength (see Palacios *et al.*, 1996, 1998 and Kraaij *et al.*, 1998). The maximal response amplitude was the largest response amplitude obtained in the measurements for that cell. The spectral sensitivity data for each cell were then shifted vertically so as to align their estimated lambda-max at log sensitivity = 0. Data from cells within individual cone types were then combined to obtain average values of relative sensitivity for each wavelength. RS is given in log units.

Results

Photocurrent responses

Individual photoreceptors, when held at a membrane potential of -60 mV under voltage clamp conditions, responded to a series of light flashes of increasing intensity with currents of increasing amplitude and duration. Representative responses of a cone photoreceptor to increasing intensities of light stimuli are shown in Figure 2.1. For a subset of all cones, time-to-peak was an average of 339 ± 90ms and flash sensitivity for a 100ms flash (in pA photons^{-1} um^{-2} flash) was 4.37 x 10^{-3} ± 2.50 x 10^{-3}, with no

significant differences between cone classes (kinetics: ANOVA, $F_{(4, 19)} = 0.590$, P=0.674; sensitivity: ANOVA, $F_{(4, 19)} = 0.156$, P=0.958, Table 2.1).

Figure 2.2 shows the current light response of one cone to various wavelengths and intensities. The resting current for this cone while clamped at -60mV was -208.4pA, and the membrane capacitance was 23.64pF. Figure 2.3 shows the intensity/response relations for the sustained part of this response for nine stimulus wavelengths. The solid lines are the Naka-Rushton function fitted through the data points (see Materials and methods). Figure 2.4 shows the normalized response amplitude function for four cones, one from each of the four spectral classes. The curve follows $r/r_{max} = I/(I + \sigma)$, where σ is the intensity for a half-maximal response (Naka & Rushton, 1966). The responses of all four cone types followed the 'Principle of Univariance', as the amplitude and shape of the response depends on the number of photons absorbed, and not the wavelength of the stimulus. Table 2.2 shows the mean electrical properties of the four cone types. The series resistance (the sum of R_{access} and $R_{pipette}$) for three of the four cone types indicates generally good quality patches at the outset of recording, but the access resistance is slightly higher than desirable in the UVS cones. Note also the mean capacitance of the UVS cones is significantly different from that of the LWS, MWS and SWS cone types ($p \leq 0.001$, Tukey HSD pair wise comparisons). Capacitance is a measure of the capacity of the cellular membrane to store charge at a given potential. The physical dimensions of the membrane are important in determining the capacitance: the more membrane, the more charge that can accumulate, therefore the capacitance is proportional to membrane surface area. The lower capacitance of the UVS cones reflects their relatively

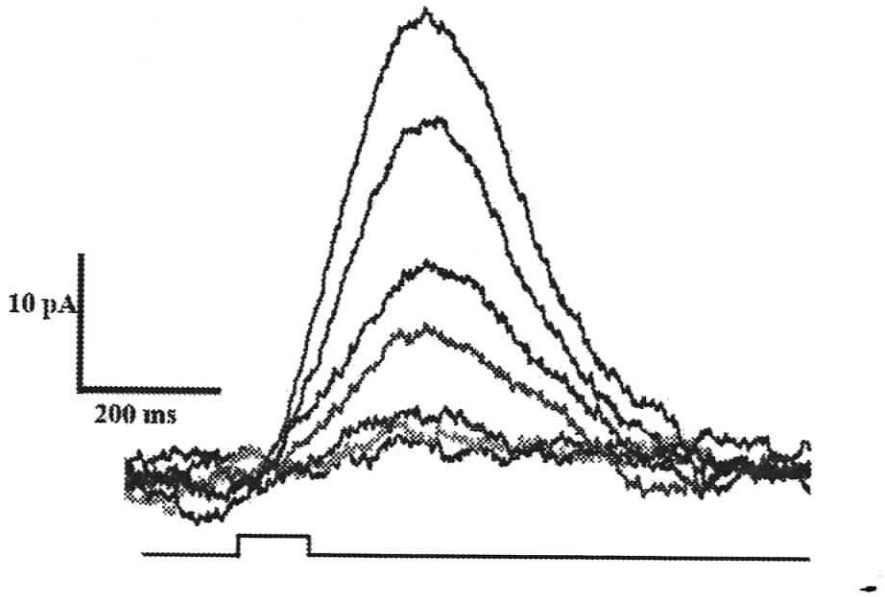

Figure 2.1: Response properties of a LWS-cone to light stimuli (560nm) of 7 intensities. Lower line indicates stimulus onset and duration (100ms). Scaling, timing and intensities are indicated in the figure.

Table 2.1: time to peak and flash sensitivities of the cones

	LWS (n=4)	MWS (n=7)	SWS (n=4)	UVS (n=5)	λ max 545nm (n=4)
Time to peak (ms)	326.98 ± 112.2	322.43 ± 74.12	374.63 ± 114.79	390.52±91.93	317.00±103.72
Sensitivity*	0.00461±0.00253	0.00473±0.00289	0.00460±0.00199	0.00377±0.00357	0.00382±0.00147

* Sensitivity = pA • photons^{-1} • μm^2 • 100ms flash; range represents ± 1 SD

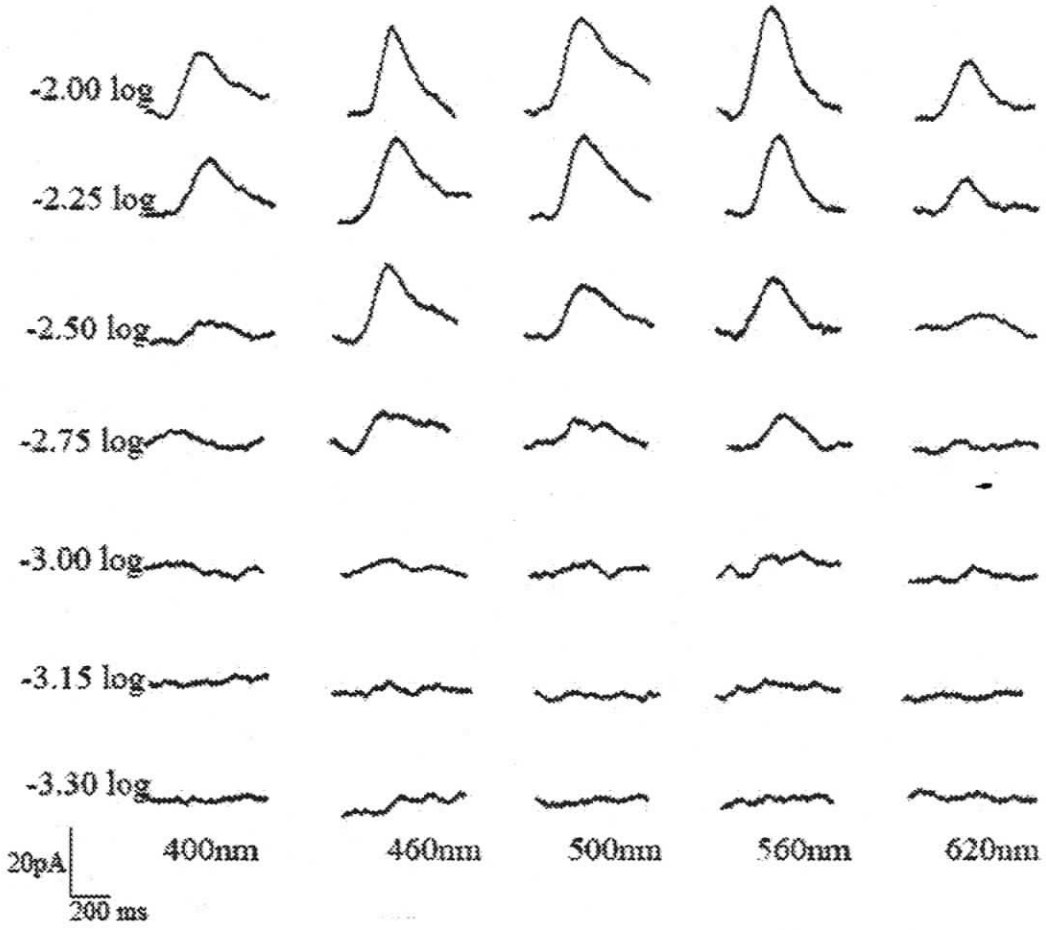

Figure 2.2: Response properties of an LWS cone to light stimuli of 5 wavelengths each at 7 intensities. For this figure, a photon flux density of 4.4×10^7 photons μm^{-2} s^{-1} corresponds to an intensity of 0 log. Scaling, timing, and stimulus wavelength are indicated in the figure.

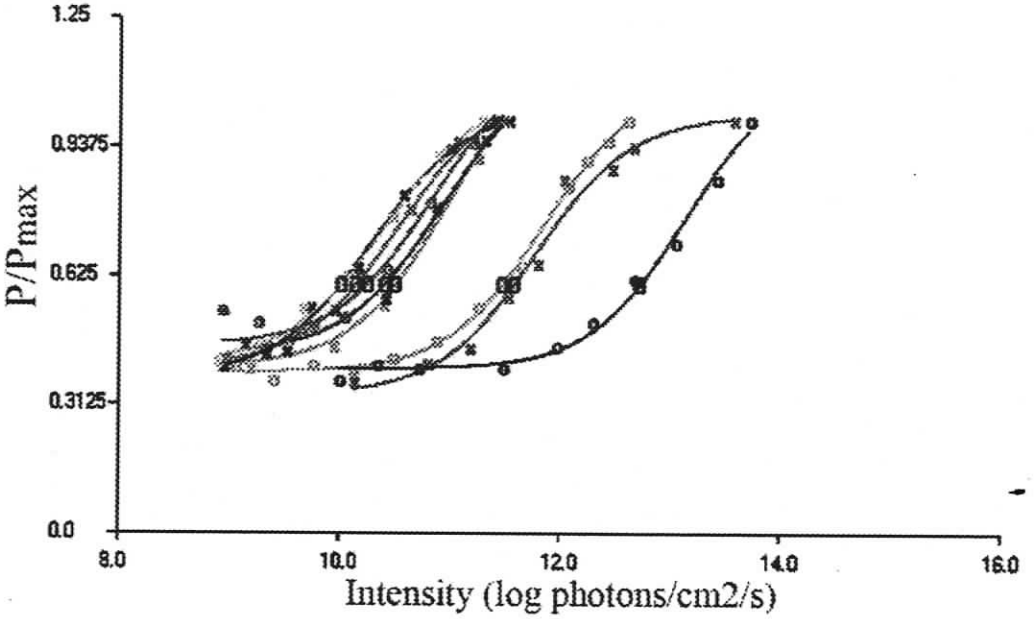

Figure 2.3: Stimulus response relation of the sustained MWS-cone light response for 9 wavelengths; each could be fitted with the same Naka-Rushton function. Open circles at 0.6 p/pmax represent the threshold criteria for that cell. Stimulus wavelengths in order of decreasing intensity are: 500, 540, 480, 580, 400, 360, 620, 330, 660nm.

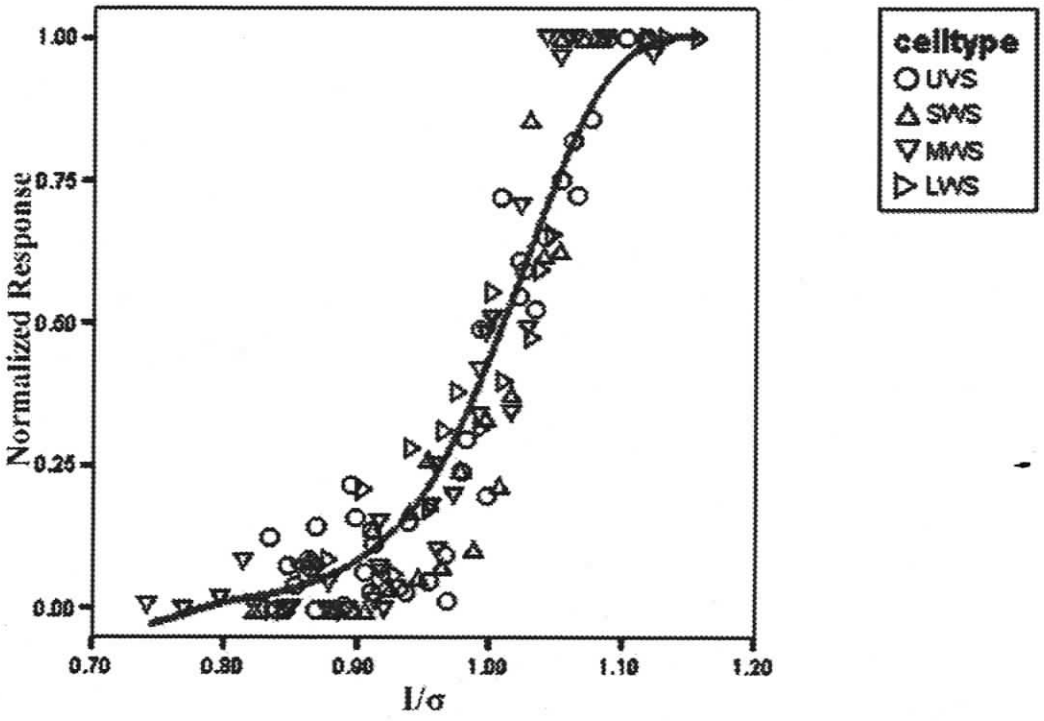

Figure 2.4: Response amplitude function from four cones (one from each spectral class). The curve follows the function $r/r_{max} = I/(I + \sigma)$, where σ is defined as I at $r/r_{max} = 0.5$.

Table 2.2: electrical properties of the cones

Parameter	LWS cones (n=15)	MWS cones (n=39)	SWS cones (n=7)	UVS cones (n=9)
I_{rest}	-317.6 ± 172 pA	-485.34 ± 288pA	-166.8 ± 138.3pA	-257 ± 207pA
C	23.79 ± 4.91pF	25.13 ± 5.64pF	20.9 ± 2.7pF	7.95 ± 5.2pF
Rm	37.42 ± 16.99 MOhm	51.30 ± 63.72MOhm	106.5±106.8 MOhm	116.2 ± 96.7 MOhm
Ra	4.50 ± 9.08 MOhm	2.00 ± 2.12MOhms	1.33 ± 1.28 MOhm	19.9 ± 6.87 MOhm
TC	66.66 ± 90.45 µs	25.63 ± 24.83 µs	17.2 ± 5.2 µs	259.41 ± 226.49 µs

I_{rest} = current flow at rest while voltage clamped at -60mV
C = mean electrical capacitance
R_m = membrane resistance
R_a = access resistance
TC = time constant
range represents ± 1 SD

small size (Figure 2.5). A general assumption used by most researchers is that a square centimeter of membrane has a capacity of 1μF (Aidley, 1998).

Analysis of the four spectral classes of cones

Figure 2.6 shows that most cells fell into one of four clusters, with λ_{max} at 373 ± 7.9, 427 ± 9, 520 ± 5.7, and 570 ± 8.5nm. A total of 108 cones were examined, 20 LWS cones, 57 MWS cones, 13 SWS cones, 14 UVS cones. Four cells with λ_{max} around 545nm did not fall within any of the four major clusters. These outliers will be considered separately below.

Figure 2.7 shows the mean normalized spectral sensitivities of the UVS, SWS, MWS and LWS cones (circles) together with the log-normalized photopigment absorption curves derived from Govardovskii et al. (2000). For the analysis of Figure 2.7, cells were only included if their λ_{max} fell within 2 S.D. of the mean, which excluded the four outlier cells noted above. The absorption curve templates were fit by eye. With the exception of the MWS cone, the spectral sensitivities follow a single photopigment absorption curve (representing 70% A_1 and 30% A_2 chromophore ratio, see Discussion) reasonably well on both the long and short-wavelength sides of their absorption spectra. The spectral sensitivity of the UVS cone is somewhat broader on the long-wavelength side, and the LWS cone deviates from the template in the region between the alpha and beta peaks. The spectral sensitivity of the MWS cone was best fit by two templates assuming different λ_{max} values (510 and 530nm), suggesting that more than one opsin may be present in the sample.

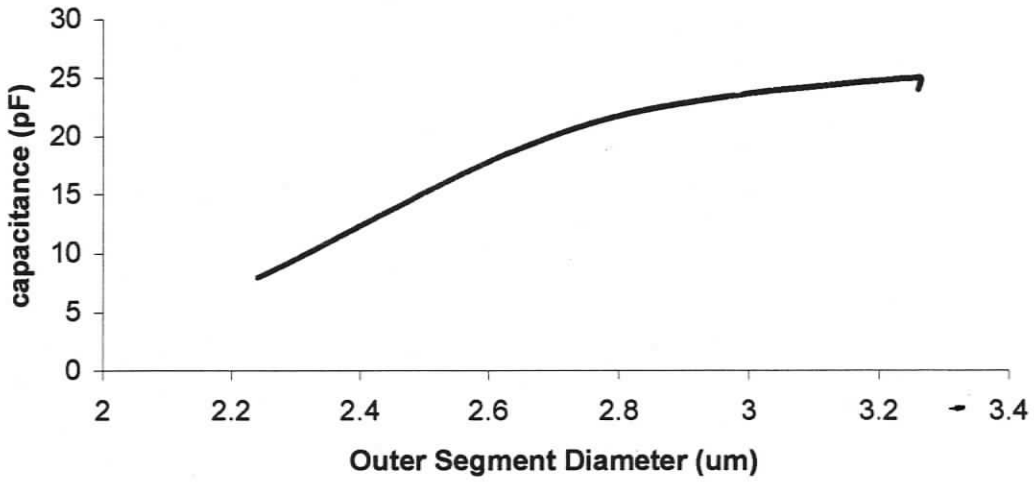

Figure 2.5: Cell capacitance (this study) as a function of cell size (mean outer segment diameter from Hawryshyn *et al.*, 2001)

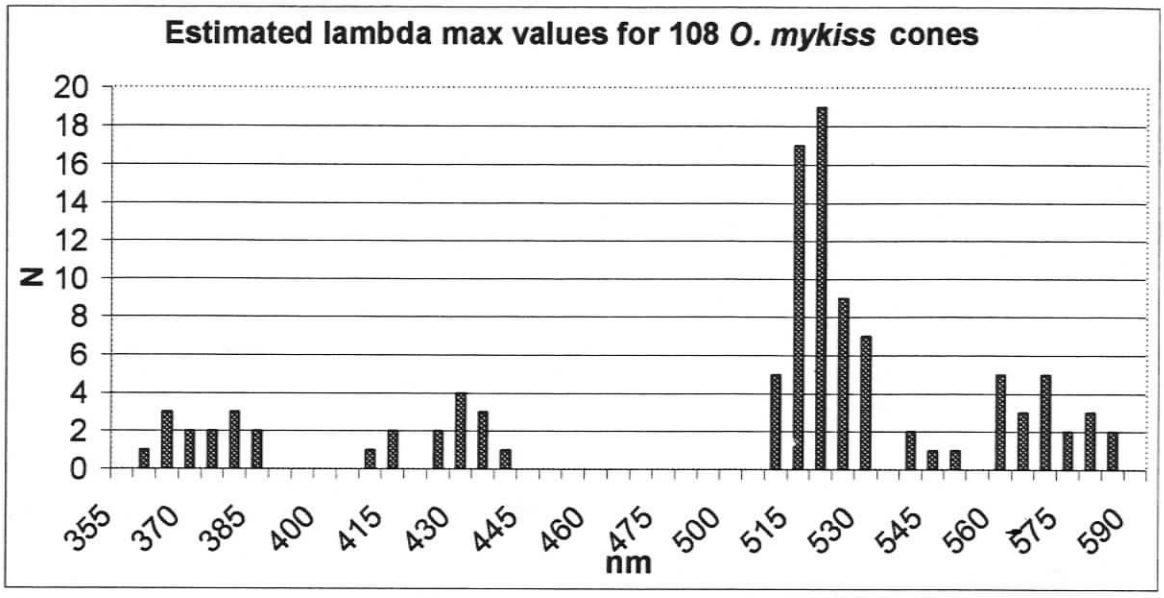

Figure 2.6: Spectral classes of 108 *O. Mykiss* cones.

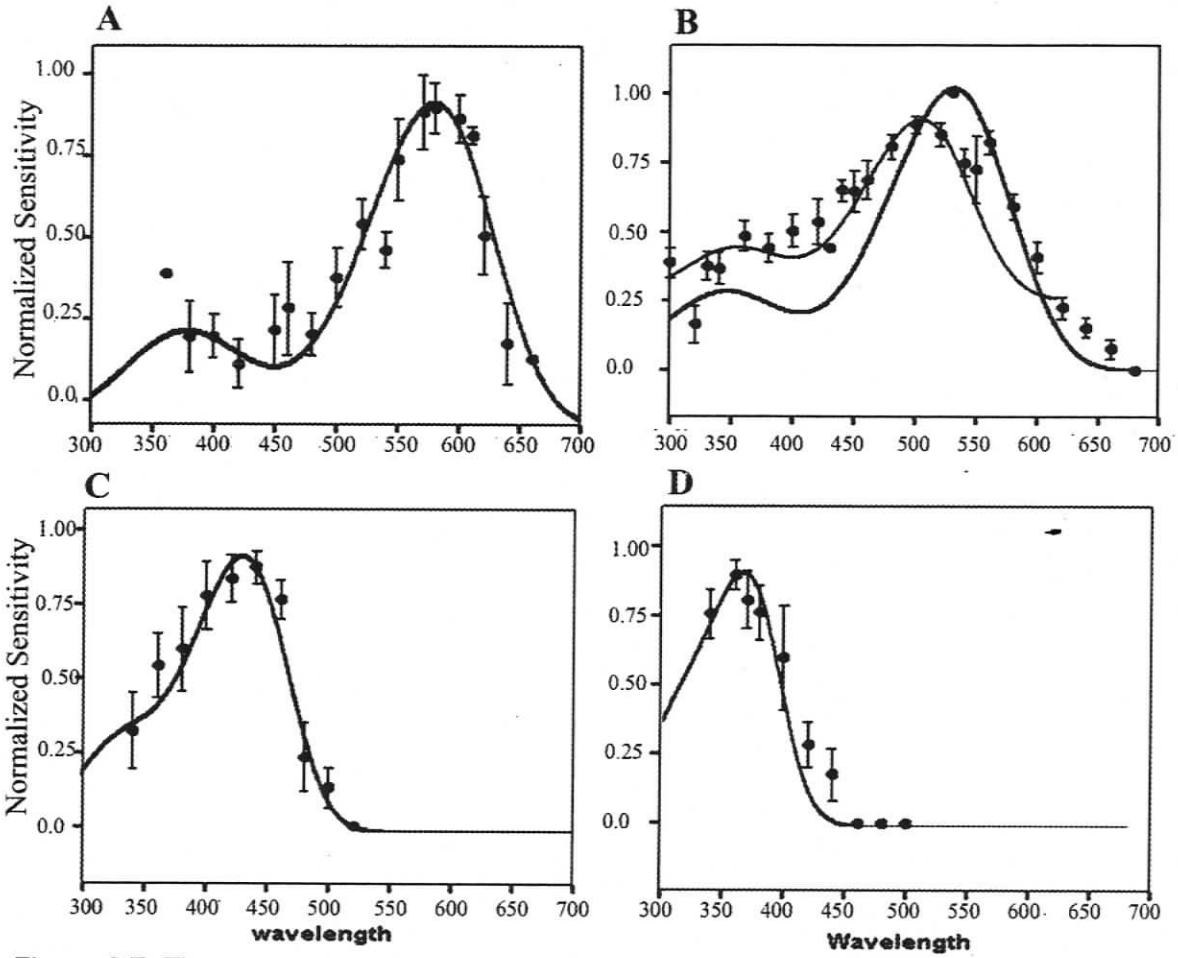

Figure 2.7: The spectral sensitivities of the (A) LWS, (B) MWS, (C) SWS and (D) UVS cones. The circles represent the action spectra determined in this study, and the solid lines are photopigment absorption curves derived from Govardovskii *et al.,* (2000) and assume an A1/A2 ratio of 70/30. Error bars represent ± 1 SD.

The half-maximum bandwidth values, in particular in comparison to those obtained from other studies of salmonids (Table 2.3), also suggest the presence of more than one opsin in the MWS cones sampled. Average data for both normalized and log relative sensitivity are given in Table 2.4. The λ_{max} values obtained for the four cone classes appear to be in good agreement with those reported in previous studies of this species (Table 2.5).

Figure 2.8 shows the pooled spectral sensitivity data for all 4 cone types plotted as a function of normalized frequency. The solid line is the template from Govardovskii *et al.,* (2000), also presented as a function of normalized frequency, and indicates that the template is a reasonable fit to the data with the exception of variance with the shorter wavelengths of the MWS cones. A comparison between the spectra of UVS photoreceptors obtained in this study and those of the giant danio (*Danio aequipinnatus*) is presented in Figure 2.9. Similar to Figure 2.6D, this figure demonstrates the UVS spectra from the present study are somewhat broader than an A_1-based visual pigment template at longer wavelengths.

Four cells with λ_{max} near 545 nm

Figure 2.10 shows data from the four cones that did not appear to belong to any of the major spectral classes (λ_{max} = 544 ± 4.8nm). Their spectral sensitivities are better fit by the dehydroretinal-based template, although they are distinctly broader than both the A_1 and A_2 templates, with HBW = 7143, suggesting that they do not represent a single cone opsin. All four cones came from different retina, and 3 of the 4 were sampled in the

Table 2.3: comparison of half-maximum bandwidth (cm^{-1}) values

UVS	SWS	MWS	LWS	species	Authors
5303	6121	7149	4054	*O. mykiss*	Present work
5051±130	4329±112	3604±62	3256±79 (3709±89)*	*O. mykiss*	Hawryshyn et al, 2001
4700±1200	6600±1500	4400±500	3700±200	*O. mykiss*	Hawryshyn and Harosi, 1994
5702±715	5092±538	4165±382	3645±326	*O. kisutch*	Cheng et al, 2006
5845±783	5119±248	4101±254	4036±203	*O keta*	Cheng et al, 2006
5915±684	5187±304	4188±265	3983±252	*O. tschawytscha*	Cheng et al, 2006
6105±831	4982±444	4201±305	3660±298	*O. gorbuscha*	Cheng et al, 2006
5902±850	5406±681	4351±306	4149±355	*Salmo salar*	Cheng et al, 2006
		4440±245		*O. kisutch*	Temple et al (in prep)

All values are means 1± SD
*values for A1 and A2 (in parentheses) based pigments

Table 2.4 Average values of normalized and log relative sensitivity at different wavelengths for the four cones of *O. mykiss*; the number of cells in each average is given in the column labeled n

	LWS cone					MWS cone					SWS cone					UVS cone				
λ	N.S.	S.E.	L.R.S.	S.E.	*n*	N.S.	S.E.	L.R.S.	S.E.	*n*	NS	S.E.	LRS	S.E.	*n*	NS	S.E.	LRS	S.E.	*n*
300	-	-	-	-	-	0.4283	0.043	-1.748	0.1815	6	-	-	-	-	-	-	-	-	-	-
320	-	-	-	-	-	0.225	0.045	-1.725	0.515	2	-	-	-	-	-	-	-	-	-	-
330	-	-	-	-	-	0.3756	0.0528	-1.823	0.1257	9	-	-	-	-	-	-	-	-	-	-
340			-	-	-	0.4233	0.02728	-1.39	0.56	3	0.3225	0.1297	-1.354	0.4263	4	0.755	0.0885	-0.685	0.2471	4
360	0.39		-0.9		1	0.49	0.0555	-0.9844	0.9725	20	0.5422	0.109	-0.5039	0.0699	9	0.8967	0.0531	-0.0333	0.9747	12
370	-	-	-	-	-	-	-	-	-	-	-	-	-	-	-	0.8057	0.1034	-0.3	0.1858	3
380	0.1967	0.1101	-0.924	0.1737	10	0.4552	0.0591	-0.8263	0.0602	25	0.5975	0.1434	-0.358	0.1171	4	0.76	0.0978	-0.2518	0.0718	11
400	0.198	0.06568	-0.956	0.1509	5	0.5	0.0608	-0.7865	0.694	24	0.7667	0.1397	-0.2159	0.1304	9	0.5967	0.1904	-0.4083	0.1132	6
420	0.1138	0.7547	-1.132	0.11417	9	0.542	0.0869	-0.7087	0.1427	15	0.8343	0.0776	-0.1806	0.06808	7	0.283	0.0815	-1.053	0.1435	10
440	-	-	-	-	-	0.6488	0.0381	-0.6775	0.0687	25	0.8738	0.0546	-0.2301	0.1254	8	0.1917	0.1043	-1.478	0.4107	6
450	0.2167	0.1093	-1.04	0.1002	3	0.698	0.0849	-0.172	0.1111	5	-	-	-	-	-	-	-	-	-	-
460	0.284	0.1441	-0.8017	0.1805	6	0.6865	0.0703	-0.4083	0.0752	23	0.765	0.0672	-0.3393	0.1203	6	0	-	-1.59		1
480	0.2044	0.063	-1.002	0.1131	9	0.8196	0.0468	-0.2836	0.0894	23	0.234	0.1161	-0.7734	0.1664	5	0	0	-1.92	0.14	2
500	0.38	0.09233	-0.7956	0.1362	9	0.9011	0.0279	-0.1331	0.0558	35	0.1314	0.0686	-1.4513	0.2403	7	0	0	-2.65	0.11	2
520	0.5418	0.0769	-0.51	0.1122	13	0.8537	0.0435	-0.116	0.0384	27	0	0	-1.7335	0.1555	2	-	-	-	-	-
540	0.464	0.0535	-0.434	0.0744	5	0.7595	0.05389	-0.3419	0.1033	22	-	-	-	-	-	-	-	-	-	-
550	0.7425	0.1248	-0.4	0.1407	4	0.724	0.1207	-0.174	0.0367	5	-	-	-	-	-	-	-	-	-	-
560	-	-	-	-	-	0.8236	0.0426	-0.2872	0.0647	11	-	-	-	-	-	-	-	-	-	-
570	0.8867	0.1133	-0.14	0.14	3	-	-	-	-	-	-	-	-	-	-	-	-	-	-	-
580	0.898	0.0768	-0.163	0.0939	12	0.5861	0.0482	-0.6847	0.0653	33	-	-	-	-	-	-	-	-	-	-
600	0.8643	0.072	-0.2288	0.1088	8	0.4072	0.0575	-1.173	0.091	25	-	-	-	-	-	-	-	-	-	-
610	0.815	0.025	-0.545	0.325	2	-	-	-	-	-	-	-	-	-	-	-	-	-	-	-
620	0.5089	0.1202	-0.632	0.1355	10	0.22	0.0409	-1.6558	0.1076	27	-	-	-	-	-	-	-	-	-	-
640	0.15	0.15	-0.9852	0.3006	3	0.1535	0.0385	-2.071	0.1095	17	-	-	-	-	-	-	-	-	-	-
660	0.33	0.3013	-1.07	0.5963	3	0.065	0.0357	-2.827	0.1695	10	-	-	-	-	-	-	-	-	-	-
680	-	-	-	-	-	0	0	-2.974	0.3153	5	-	-	-	-	-	-	-	-	-	-

Table 2.5: comparison of photopic λ_{max} values obtained from electrophysiological, microspectrophotometric and behavioural observations of *O. mykiss* (nm)

UVS	SWS	MWS	LWS	Authors	Method
373	427	520	570	Present work	WPC
370-380	440	540	580	Parkyn & Hawryshyn, 2000	GCR
390	420	510	NE	Beaudet et al., 1993	GCR
371	432	519	574(623)*	Hawryshyn et al., 2001	MSP
400	453	530	598	Kusmic et al., 1993	MSP
365	434	531	576	Hawryshyn and Harosi, 1994	MSP
NE	440	535	630	Douglas, 1993	Behaviour
360	430	540	620	Hawryshyn et al., 1989	Behaviour

WPC, whole-cell patch clamp; GCR, ganglion cell responses; MSP microspectrophotometry; NE not examined; *values for A1 and A2 (in parentheses) based pigments

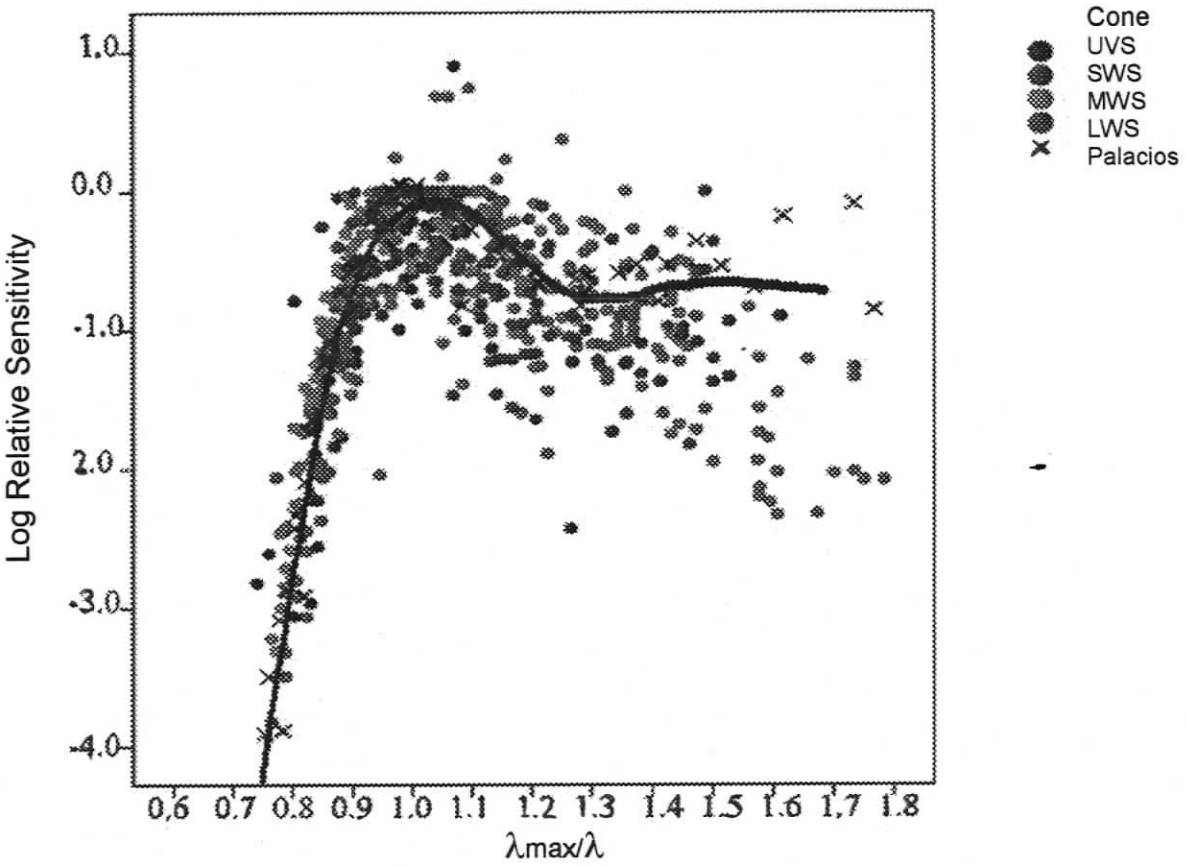

Figure 2.8 Pooled data for the spectral sensitivity of the all cone photoreceptor types from this study (108 *O. mykiss* cones) plotted as a function of normalized frequency. X marks data points from Palacios et al., 1996 for UVS photoreceptor. The solid line is the Govardovskii *et al.,* (2000) based template for A_1-based pigments, also plotted as a function of normalized frequency.

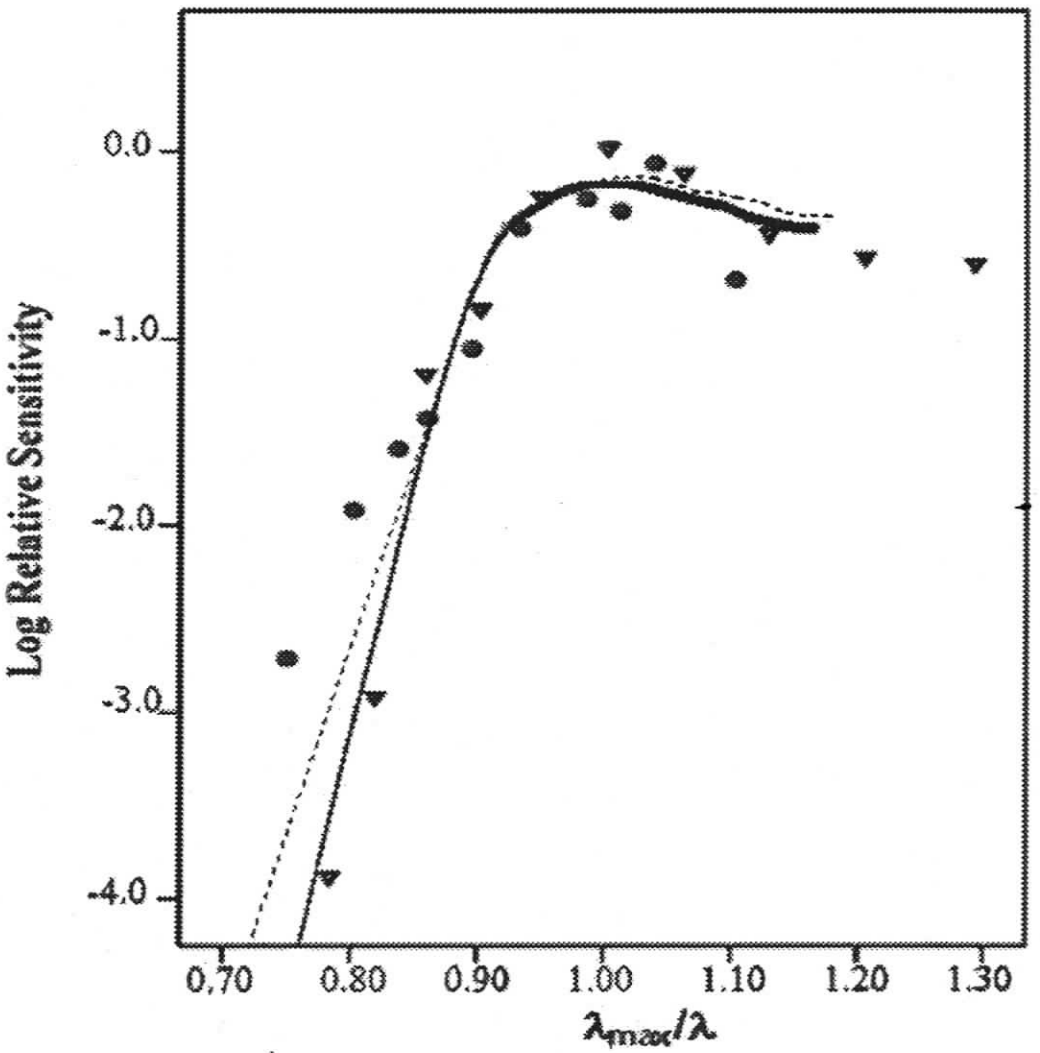

Figure 2.9: Normalized frequency plot of UV receptors. Circles: spectral sensitivity of *O. mykiss* (present work); triangles: spectral sensitivity of giant danio cones (*Danio aequipinnatus*) from Palacios *et al.*, (1996). Curves are based on Govardovskii *et al.*, (2000) also plotted as a function of normalized frequency, with the solid curve representing 100%A1; and the dashed curve representing 70%A1 and 30%A2.

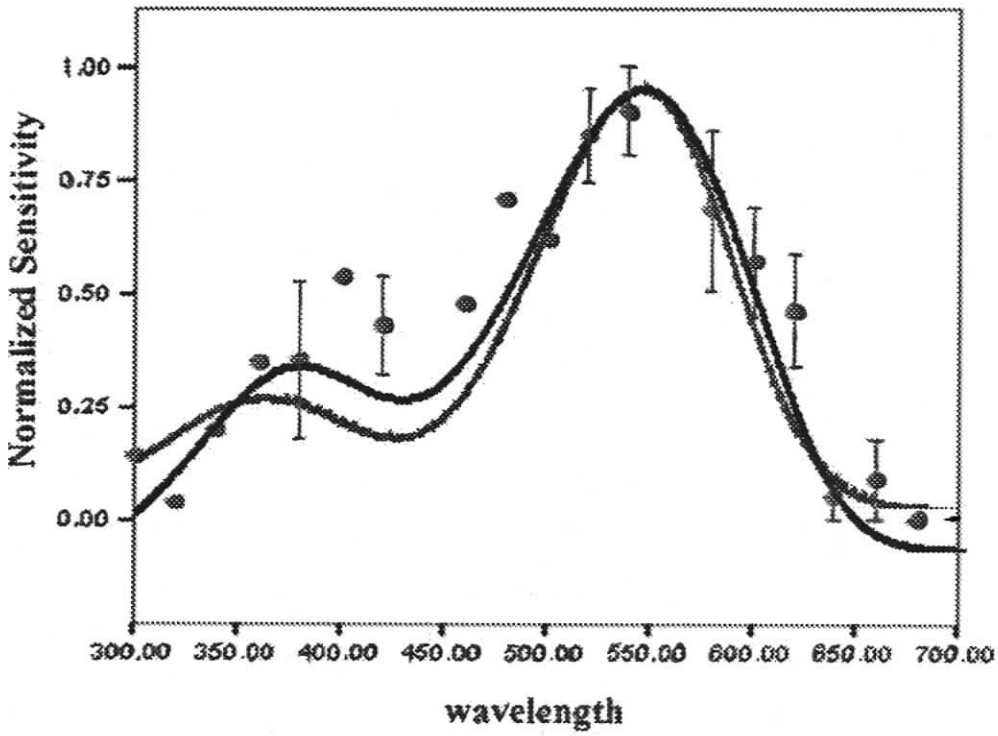

Figure 2.10. Four cones with lambda-max estimated at 544 ± 4.8 that did not belong to any of the major spectral classes. Solid curve: template for A_2-based pigments; dotted curve: equivalent template for A_1 based pigments. Error bars represent ± 1 SD.

latter part of the data collection (late November and December, 2005). Each of these retina had other cones sampled (2 UVS, 2 MWS and 2 LWS) that fell within 2 SD of the λ_{max} estimated for the various cone classes.

Discussion

Comparison with earlier work on different spectral cone classes

Whole-cell patch-clamp recordings from intact cone photoreceptors in an isolated retina preparation have permitted measurement of cone spectral sensitivity in rainbow trout. The cone pigments of *O. mykiss* have been previously measured by MSP and behavioural methods and the results are summarized in Table 2.5. The results of this study are generally in good agreement for all four cone classes. The variations in λ_{max} among the studies may reflect differences in measurement techniques, mode of analysis and ratios of A1:A2 chromophores or the presence of opsin subtypes. Physiological measures of spectral sensitivity may have an advantage over microspectrophotometry in determining λ_{max} because of the additional information present on the long wavelength side of the α-band. However, MSP has the advantage of producing essentially continuous sets of data which can be accumulated over a much shorter period of time, allowing improvement in the data by averaging and reducing the likelihood of variations in the ratio of A_1:A_2 chromophores (see Discussion below).

Fit of cone spectra to a common absorbance template

Two of the four receptor types (UVS and MWS) have broader than expected spectral sensitivity (Figures 2.7 and 2.9). Possible sources of this variance include a higher than expected percentage of the A_2 chromophore and the presence of more than one opsin.

- *Variations in the ratio of A_1/A_2 chromophores*

Vertebrate visual pigments consist of two main components: an opsin (protein) and a prosthetic group, or chromophore, derived from either vitamin A_1 (retinal) or A_2 (3,4-dehdyroretinal). The spectral absorption properties of the visual pigment, including the wavelength of maximum absorption (λ_{max}), are determined primarily by the opsin, and variations in the amino acid sequence result in the different classes of vertebrate opsins (e.g. ultraviolet, short, middle and long wavelength-sensitive opsins, and rod opsins). Some species, including most salmonids, have a mix of A_1 and A_2 chromophores in their retina (Munz and Beatty, 1965; Beatty, 1966) and many species of salmonids are capable of shifting between A_1 and A_2 chromophores (Dartnall and Lythgoe 1965; Beatty, 1966, Alexander *et al.,* 1994; Allen *et al.,* 1973; Allen and Munz, 1983, Temple *et al.,* 2006). Two consequences of shifting from A_1- to A_2-based chromophores in the same opsin are shifting the λ_{max} of the visual pigment to a longer wavelength and broadening spectral bandwidth of absorbance (HBW, half-band width) (Wald and Brown 1953; Brown *et al.,* 1963; Bridges 1967). The relative amounts of the two chromophore types have been found to vary by species and to be dependent on life cycle in relation to migration, time of year and extrinsic factors such as photoperiod, temperature and thyroxine (Tsin and Beatty, 1977, McFarland and Allen, 1977, Tsin, 1979; Temple *et al.,* 2006).

Visual pigments with λ_{max} values at longer wavelengths experience larger shifts in their λ_{max} when an A_1-based chromophore is replaced by an A_2-based chromophore (Bridges 1965; Dartnall and Lythgoe 1965; Tsin *et al.,* 1981; Whitmore and Bowmaker 1989; Harosi 1994; Parry and Bowmaker 2000). The difference is small in the violet region of the spectrum, about 20nm for rods or mid-wavelength cones, and increases to more than 60nm for long-wavelength cones (Tsin and Beatty, 1978; Whitmore and Bowmaker, 1989). Therefore, the LWS data set should be the best predictor of A_1/A_2 ratio. Although the estimated HBW for the LWS cones in this study is relatively high compared to other reports (Table 2.3), the estimated λ_{max} is more consistent with that of an A_1-dominant retina (Table 2.5). The template that best fits the LWS spectral sensitivity curve is based on 70/30 A_1/A_2 which is near the upper limit of A_2 that is likely for this species (Temple *et al.,* 2006, Hawryshyn *et al.,* 2001, Hawryshyn and Harosi, 1994; Beatty, 1966; Munz and Beatty 1965; Allen *et al.,* 1973, 1982). The 70/30 A_1/A_2 template also fits the SWS and UVS cones reasonably well, although it is slightly narrower than the UVS results on the long wavelength portion of the spectrum and substantially narrower than the MWS results. The HBW for the UVS cones obtained in this study is comparable to that measured in previous studies, but the large HBW measure for the MWS cones combined with an unsatisfactory fit of a template based on 100% A_2-chromophores (not shown) indicates that variations in A_1/A_2 ratio alone cannot account for the breadth of the MWS spectral sensitivity results.

- *Possible influence of opsin subtypes*

Until recently, classes of cone photoreceptors within a species were commonly assumed to contain a single opsin type. Recent research has demonstrated that more than one opsin subtype may be expressed not only within a class of photoreceptors but within

individual photoreceptors (Archer and Lythgoe, 1990; Cheng *et al.,* 2005); Previous research has proposed the presence of multiple opsins within a cone class on the basis of spectral sensitivity spectra that are broader than the template (Makino and Dodd, 1996, Palacios *et al.,* 1998; Govardovskii *et al.,* 2000). In *Oncorhynchus* spp. it has been shown that the single UVS and SWS cones express the SWS1 And SWS2 opsin classes while the two outer segment members of double cones express RH2 and MWS/LWS opsin classes (Allison *et al.*, 2003). Recent MSP investigations of visual pigments in *Oncorhynchus* spp identified a range of λ_{max} values in MWS cones that was greater than could be explained by a single opsin and variable A_1/A_2, which led to the identification of a second RH2 opsin subtype (Temple, 2006). The presence of a mix of the RH2A and RH2B opsins in MWS cones sampled in this study would adequately account for the shape of the spectral sensitivity spectrum obtained.

- *Four outliers*

There were four cells with λ_{max} at about 545nm that did not appear to fall into any of the other spectral classes. As shown in Figure 2.10, the width of the α-band is more consistent with an A_2-chromophore, although neither a retinal nor dehydroretinal-based template provides a satisfactory fit to the data. Unlike previous reports in striped bass (*Morone saxitilis,* Miller and Korenbrot, 1993) and giant danio (*D. aequipinnatus*, Palacios *et al.,* 1996) this set of cones does not appear to represent a second class of either the MWS or LWS cone types as there is no apparent difference in the kinetics or sensitivity when compared to any of the four cone classes in this study (Table 2.1). The lambda max values of these cones fall within the expected range of the RH2B opsin subtype (Temple, 2006) and may provide additional evidence of the presence of more than one opsin subtype in the MWS data set as discussed above.

- *Implications for investigations of neural pathways*

The protocols developed for this study can now be applied to the investigation of processing of UVS and polarization sensitivity both within photoreceptors and between photoreceptors and second order neurons. Characterizing the spectral sensitivity of the feedback signal from horizontal cells to cones resulting from UV stimuli is an important step in the development of research related to both colour processing and polarization sensitivity (see Chapter 3).

It is unclear whether an isolated retina preparation can be used in direct assessments of polarization sensitivity, as one hypothesis for the basis for the selective absorption of electric-vector (e-vector) orientations of polarized light proposes that polarization sensitivity is mediated by the geometry of the square cone mosaic of salmonids (Novales-Flamarique *et al.,* 1998). However, other biophysical models of e-vector absorption (Roberts *et al.*, 2004) which do not depend on the geometric relationships among cones, combined with recent evidence indicating that the detection of differentially polarized light stimuli is not dependent on the presence of corner cones (Hawryshyn *et al.,* 2003) suggest that it may be possible to use an isolated retina to directly assess polarization sensitivity.

Chapter 3: Retinal processing and opponent mechanisms mediating ultraviolet polarization sensitivity

This chapter is based on a collaboration with the following authors and is in preparation for submission to the Journal of Experimental Biology as cited below:

S.D. Ramsden, L.G. Anderson, M. Mussi, M. Kamermans and C.W. Hawryshyn (in prep). Retinal processing and opponent mechanisms mediating ultraviolet polarization sensitivity.

Introduction

The visual world of fish is a complex environment, where colour, intensity and polarization of light are available to guide behaviours (Cronin and Shashar, 2001; Parkyn *et al.*, 2003; Novales Flamarique and Hawryshyn, 1997; Gal *et al.*, 2001; McFarland and Munz, 1975a; Pomozi *et al.*, 2001). The complexity of the underwater photic environment is mirrored by the diversity of visual adaptations that have evolved to perceive these qualities of light (Barry and Hawryshyn, 1999; McFarland and Munz, 1975b; Novales Flamarique and Hawryshyn, 1993). Many species of fish have also evolved visual mechanisms for the perception of linearly polarized light and behaviours based on this perception, (Hawryshyn and McFarland, 1987; Hawryshyn *et al.*, 2003; Parkyn and Hawryshyn, 2000; Parkyn *et al.*, 2003; Shashar *et al.,* 1996; 1998; 2001; Shashar and Hanlon, 1997; Waterman and Hashimoto, 1974) but little is known about the neuronal mechanisms underlying these abilities.

A number of techniques have been used to examine polarization sensitivity (PS) in a broad range of teleost species including: heart rate conditioning (Hawryshyn and McFarland, 1987), single unit recording from the *torus semicircularis* (Coughlin and Hawryshyn, 1995) and the optic tectum (Waterman and Hashimoto, 1974), compound action potential recordings from the optic nerve (CAP) (Parkyn and Hawryshyn, 1993; 2000), electroretinograms (ERG) (Hawryshyn *et al.*, 2003) and behavioural orientation and discrimination paradigms (Hawryshyn *et al.,* 1990, Parkyn *et al.*, 2003; Degner and Hawryshyn, 2001; Mussi *et al.*, 2005). Within teleosts however, examinations of the neuronal pathways underlying PS have been restricted to a few species and mainly through the use of techniques such as single unit and CAP recording (see Hawryshyn, 2000 for review).

CAP recordings by Parkyn and Hawryshyn (1993; 2000) identified horizontal and vertical polarization detector mechanisms by examining the PS of the four cone mechanisms isolated through chromatic adaptation. Briefly, these experiments, like those performed on goldfish (Hawryshyn and McFarland, 1987), demonstrated that ultraviolet-sensitive cone (UVS) mechanism mediated vertical PS, while the medium and long wavelength-sensitive cone mechanisms (MWS and LWS) mediated horizontal PS. When a spectrally broad background is used in conjunction with UV linearly polarized stimuli, PS curves show a "W-shaped" PS function. Peak PS occurs at 0° and 90° representing the combined presence of the vertical and horizontal polarization detector mechanisms. A full description of these observations is provided in Parkyn and Hawryshyn (1993) and Coughlin and Hawryshyn (1995).

A recent study using ERG recordings to examine the PS of three species of damselfishes (Hawryshyn *et al.,* 2003) identified more complex PS curves (four peaks) than the two-channel W-function commonly found in salmonids using CAP recording. As the evaluation of PS in salmonids using the ERG technique had not previously been attempted and since ERG and CAP recordings reflect two different levels of processing polarization information, early and late retinal processing respectively, I was interested in using ERG recording to evaluate PS.

The aim of this study is to determine where the critical coding step or steps for polarization vision are performed. The sensitivity to polarized light was determined at two locations: 1) at the output stage of the retina by recording compound action potentials (CAP) in the optic nerve and 2) at the input stage of the retina by recording the electroretinogram (ERG). The spectral sensitivity of the various components of the responses was determined using chromatic adaptation techniques, and the underlying neuronal mechanisms were studied using a pharmacological approach.

Materials and Methods

Animals and holding conditions

Juvenile rainbow trout (*Oncorhynchus mykiss*) between 5-10 g body mass were obtained from the Fraser Valley Trout Hatchery, Abbottsford, B.C., Canada. Fish were held on a 12L:12D photoperiod and maintained at 15+/-1°C. All surgical procedures were conducted between 08:00 and 18:00 hrs to obviate any effects related to diel retinomotor movements (Parkyn and Hawryshyn 1993; 2000). The photic conditions within the holding facility were provided by full spectrum fluorescent lamps (6500°K). All experimental procedures and animal care were approved by the University of Victoria Animal Care Committee under the auspices of the Canadian Council for Animal Care.

Preparation of Fish

Experimental preparations for both electroretinogram (ERG) and compound action potential (CAP) recordings are described elsewhere in detail (Beaudet *et al.*, 1993; Hawryshyn *et al.*, 2003; Parkyn and Hawryshyn, 2000). In brief, rainbow trout were immersed in a solution of 125 mg · L^{-1} tricane methanesulphonate (MS-222) until the fish reached stage IV anaesthesia (Joly *et al.*, 1972). Standard length (cm) and body mass (g) were measured. Sub-cuteaneous injections of a general anaesthetic, Maranil (0.005 mg · kg^{-1} body weight) and an immobilizing agent, pancuronium bromide (0.05 mg · g^{-1} body weight) were administered at several sites. The test fish were then placed in a restraining cradle in a faraday cage. Experimental fish were irrigated with aerated water (10°C, flow rate of approximately 3 ml s^{-1}) and the body covered with moist cloth. For CAP experiments, the dermis overlying the right frontal bone was removed with a scalpel

and surgical drill holding a dental burr. This provided access to the right rostral optic tectum through which the recording electrode was advanced into the optic nerve.

Experimental Apparatus

The optical system and recording apparatus has been described previously (Hawryshyn *et al.,* 2003; Parkyn and Hawryshyn, 2000). Two background channels using 250 W quartz-halogen lamps (USHIO) were used for providing constant background fields and chromatic adaptation. Long and short wavelength cut-off interference filters, Schott colour filters and neutral density filters/wedge were used to manipulate both the energy and wavelength distribution of each background channel. A quantum catch model was employed to determine filter combinations necessary to produce the desired background conditions. A bifurcated fiber optic (fused silica, na=0.22, Fiberoptic Systems) was used to superimpose the background channels onto the eye. The stimulus channel used a 300 W xenon arc lamp system (Oriel). The optical path consisted of a monochrometer (Instruments SA), Inconel quartz neutral density wedge (0-4.0 neutral density; Melles-Griot), shutter (Uniblitz, Vincent Associates) and optical filters to block spectral sidebands, and UV optics to match the numerical aperture of the liquid light pipe (na=0.74). The stimulus and background illuminated the left eye of the fish. Both the stimulus and background fields were spatially broad to mimic natural celestial and underwater-polarized light conditions. Spectral sensitivity was measured in 20 nm increments from 360 to 620 nm using a staggered wavelength presentation to prevent adaptation to a certain region of the spectrum.

For PS measurements, a UV-transmissive linear polarizer (HNP'B, Polaroid) (manually adjusted) was placed over the ferrell of the liquid light pipe. Measurements were randomized from 0° to 180° in 15° increments, where the 0°/180° e-vector axis was defined as vertical relative to the gravitational axis of the fish and 90/270° was defined

as horizontal (Hawryshyn and McFarland, 1987). Fish were light adapted with unpolarized light from the background channels, and a plane-polarized, 360 nm stimuli, in 0.2 log unit increments steps, was used to measure UV PS. The use of two light pipes, one for the stimulus and the other for the background obviated e-vector adaptation from the background channel. A quantum catch model was used to generate photic conditions aimed at carefully controlling the level of light adaptation of the respective cone mechanisms:

$$Q_i = \int A_i(\lambda)G(\lambda)d(\lambda) \qquad (1)$$

where $Q_i(\lambda)$ denotes the quantum catch of receptor (i), $A_i(\lambda)$ denotes the visual pigment absorption coefficient of receptor (i), and $G(\lambda)$ denotes the photon irradiance (spectral energy distribution) of the background light field. Integrations were performed for each receptor mechanism between 300-800 nm for the various background conditions considered. This assessment, in addition to cone mechanism light adaptation dynamics (Hawryshyn, 1991), allowed us to finely control the state of adaptation of the cone mechanisms. Such considerations were essential to avoid complete suppression of either the UVS or LWS cone mechanisms. The following background adaptation conditions were used: (i) *White Light Background* – 700 nm short pass (SP) plus 2.0 neutral density filters in each background channel (1 and 2); (ii) *LWS cone mechanism adaptation* – 600 nm long pass (LP) and 1.5 neutral density in channel 1, and 700 nm SP and 2.0 neutral density filters in background channel 2; (iii) *UVS cone mechanism adaptation* - UG-11 and 1.3 neutral density filters in channel 1, and 700 nm SP and 2.0 neutral density filters in channel 2. Spectral energy distribution curves are shown in Figure 3.1 (see Table 3.1 for quantum capture calculations).

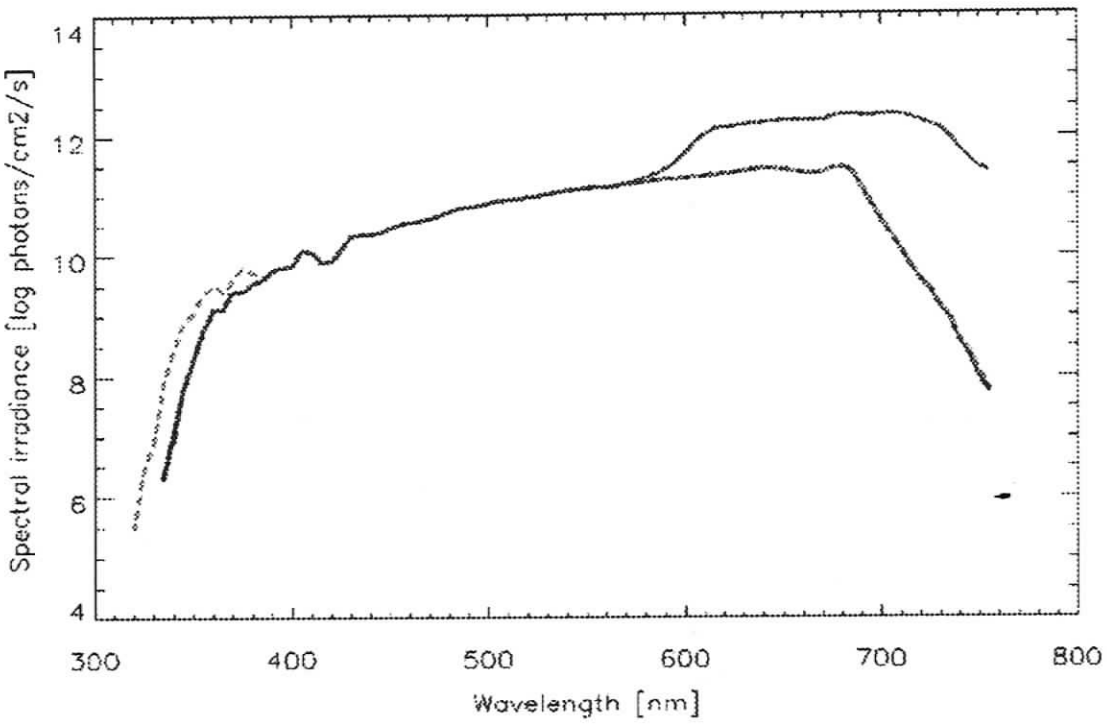

Figure 3.1: Spectral energy distribution of the adapting backgrounds. The irradiance measurements are plotted in log irradiance (photons • cm^2 • s^{-1}). The solid black line represents the broad-spectrum tungsten halogen adapting background used in control and cobalt PS and spectral sensitivity experiments. The solid red line depicts the LWS cone mechanism adapting condition using a 600LP cutoff filter, while the solid blue line represents the UVS cone mechanism adapting condition using a UG-11 filter in a tungsten halogen background channel.

Table 3.1 Quantum capture calculations for background adaptation conditions.

	Quantum catch (photons/cm^2/s)			
	UVS cones	SWS cones	MWS cones	LWS cones
Control	3.92×10^{10}	3.69×10^{11}	2.06×10^{12}	3.89×10^{12}
LWS cone adapting	3.92×10^{10}	3.69×10	2.45×10^{12}	1.09×10^{13}
UVS cone adapting	5.27×10^{10}	4.19×10^{11}	2.19×10^{12}	4.04×10^{12}

Intraocular Injections

Previous research has shown that sub-millimolar concentrations of cobalt block the horizontal cell feedback induced responses of cones in turtle (Thoreson and Burkhardt, 1990; Vigh and Witkovsky, 1999) and in fish (Fahrenfort *et al.*, 2004). Injections of either cobalt chloride (Sigma-Aldrich) or saline were made at the limbus of the left eye using a 30-gauge needle. Final concentrations of cobalt were estimated following the method used by Demarco and Powers (1989). In short, the average volume of vitreous was estimated to be 145 μl, and 10 μl of 4.26 mM cobalt chloride was injected, resulting in a final estimated ocular concentration of 0.275 mM. This estimate represents a first order approximation of the cobalt chloride concentration in the eye and may not reflect what is actually present in the outer retina at the time of the measurements (i.e. this value may not be directly comparable to concentrations delivered to isolated retina or eyecup preparations superfused with physiological medium and pulsed with cobalt chloride).

Recording Procedure: ERG

A glass electrode (1mm ID, loaded with seawater (28ppt)) was inserted into a saline filled half-cell (A-M systems), and the tip was positioned using a micromanipulator on the dorsal-nasal surface of the left eye. A ground electrode was attached to the caudal fin and a chlorided-silver reference electrode was placed in the right nares of the test fish. Fish were acclimated for 45 mins. prior to experiments using chromatic adaptation or cobalt treatments. A Grass Hi-Z probe (Grass-Telefactor) provided the input to a Grass instruments P-5 preamplifier (bandpass filter settings, 0.3 Hz low-pass and 300 Hz high-pass). The amplified signal was analyzed with a 16-bit A/D data acquisition board (National Instruments, Inc.). A custom designed software analysis

module determined the b-wave amplitude by measuring the change in potential from the peak a-wave to peak b-wave during the period 150 ms post stimulus onset. The stimulus duration was 500 ms with an inter-stimulus interval of 20 s.

Recording Procedure: CAP

A sharpened Teflon coated chlorided-silver electrode (0.5mm diameter, 0.5mm exposed tip) was inserted into the optic nerve of the left eye using a micromanipulator following procedures used by Parkyn and Hawryshyn (1993; 2000). Correct placement of the recording electrode into the optic nerve was critical since Coughlin and Hawryshyn (1995) demonstrated that optic tecta do not possess UV polarization-sensitive neurons. To avoid misplacement of the recording electrode, a custom designed stereotaxic apparatus was used. Further, the waveform recorded in response to photic stimuli differs between tectal and optic nerve location of the electrode tip (see Parkyn and Hawryshyn, 2000). Post mortem dissections verified the correct trajectory and placement of the electrode. Ground and reference electrodes were placed on the fish as described above.

Data acquisition of "ON" optic nerve compound action potential responses was determined by comparing the baseline noise amplitude 50 ms prior to stimulus onset with the response amplitude 50 ms post stimulus onset.

Analysis of ERG and Optic Nerve Responses

Response versus intensity (RI) curves for each wavelength and e-vector combination were generated and statistically fitted with a third order polynomial function. A criterion response was selected to intersect within the linear dynamic range of the RI curve and normally set at 20 μV above the base line noise. Threshold intensities were interpolated from RI curves using the 20 μV response criterion. Threshold intensity

values were normalized between 0-1 to remove differences in absolute sensitivity between individuals.

The input signals were taken as the logarithmic response of the polarization detectors:

$$V = \log_{10}(\cos^2 * (\alpha)), \quad (2)$$

$$H = \log_{10}(\sin^2 * (\alpha)), \quad (3)$$

where V and H designate the response of the vertical and horizontal detector mechanisms, α is the polarization angle of the incident light (0-180°). A linear subtractive model was used to examine the opponent interactions between the V and H polarization detector mechanisms:

$$S_v = (k_1 * V) - (k_2 * H) \quad (4)$$

$$S_h = (k_3 * H) - (k_4 * V) \quad (5)$$

where S_v is the sensitivity of the vertical detector mechanism with the amplitude of inhibitory influence of V and H set by weighting factors k_1 and k_2, and S_h is the sensitivity of the horizontal mechanism with the amplitude of inhibitory influence of V and H set by weighting k_3 and k_4.

Results

Waveforms and response versus intensity curves

Figure 3.2 illustrates representative ERG and CAP waveforms in response to 500 ms flashes of 360 nm linearly polarized light of various intensities. The waveforms have been vertically displaced for presentation clarity and represent responses to 0.2 log unit increments in stimulus intensity with the lowest intensity at the base of the plot.

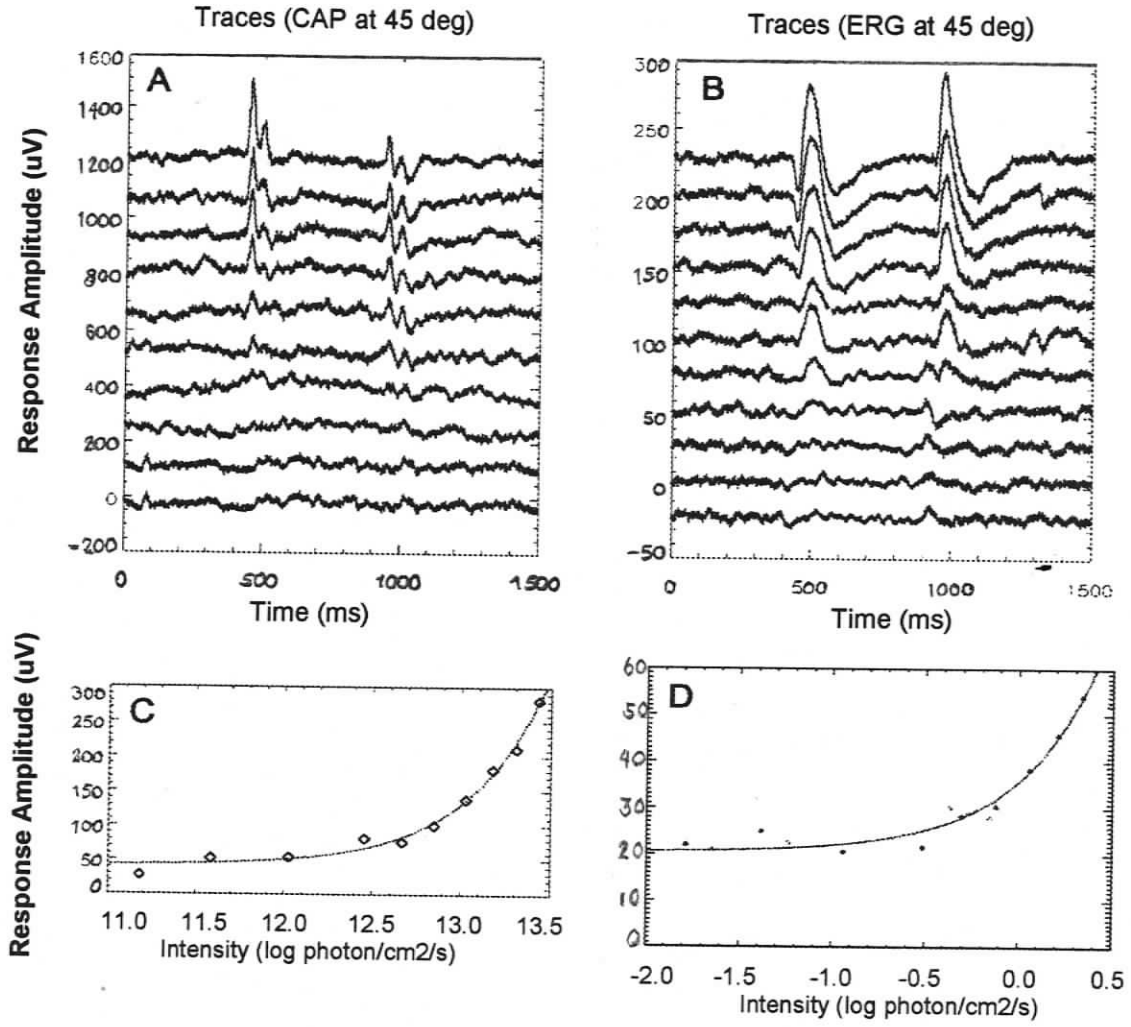

Figure 3.2 Waveforms and response versus intensity curves for compound action potential and electroretinogram recording. A CAP waveforms ("ON" responses) at increasing intensities. Note that individual traces for Fig. 2 A, B were vertically displaced for clarity of presentation. Intensity was incremented in 0.2 log unit steps of a 360 nm linearly polarized stimulus with an e-vector orientation of 45°. B ERG waveforms at increasing intensities recorded from a control fish (sham control, intraocular injection of saline). C Response versus intensity curve based on CAP data taken from panel **A**. D Response versus intensity curve based on ERG data taken from panel **B**.

Intensity response curves (see Materials and methods) were constructed and the intensities needed to obtain a criterion response of 20 uV were determined. The inverse of the intensity was defined as sensitivity. CAP recordings in the optic nerve shown in Fig. 3.2A were comparable to those observed in our previous studies (e.g. Parkyn and Hawryshyn, 2000). Optic nerve recording waveforms exhibited ON and OFF responses. The ON response amplitudes were plotted against stimulus intensity to illustrate the response dynamics of ganglion cell axons in the optic nerve. Note that only ON responses were used in this analysis as previous studies (e.g. Parkyn and Hawryshyn, 2000) have shown that they represent the activity of each of the cone mechanisms (UVS, SWS, MWS, LWS) in salmonids, while OFF responses reflect the activity of the MWS cone mechanism only. The response versus intensity curve is shown in Figure. 3.2c. The ERG recordings shown in Fig. 3.2b share the same graphical format as Fig. 3.2a. At higher intensities, the control ERG waveforms show the classical components (a-, b-, c-, and d-waves, Brown, 1968). The b-wave amplitude of ERG recordings was used to determine PS The intensity response relationship is shown in Figure 3.2d.

Spectral sensitivity

Chromatic adaptation experiments were performed to study the contribution of the various cone systems to the vertical and the horizontal polarization mechanisms. Background light conditions were selected to light adapt either the UVS cone mechanism (using a UG-11 filter) or LWS cone mechanism (using a 600nm long-pass filter). Figure 3.3 shows that, as expected, adaptation of the UVS cone mechanism leads to a reduction of the sensitivity in the short wavelength part of the spectrum (below 450 nm) and that LWS cone mechanism adaptation leads to a reduction of sensitivity in the long wavelength part of the spectrum. The background stimuli were adjusted to exert relatively minor changes in the adaptational state of the cone mechanisms, resulting in

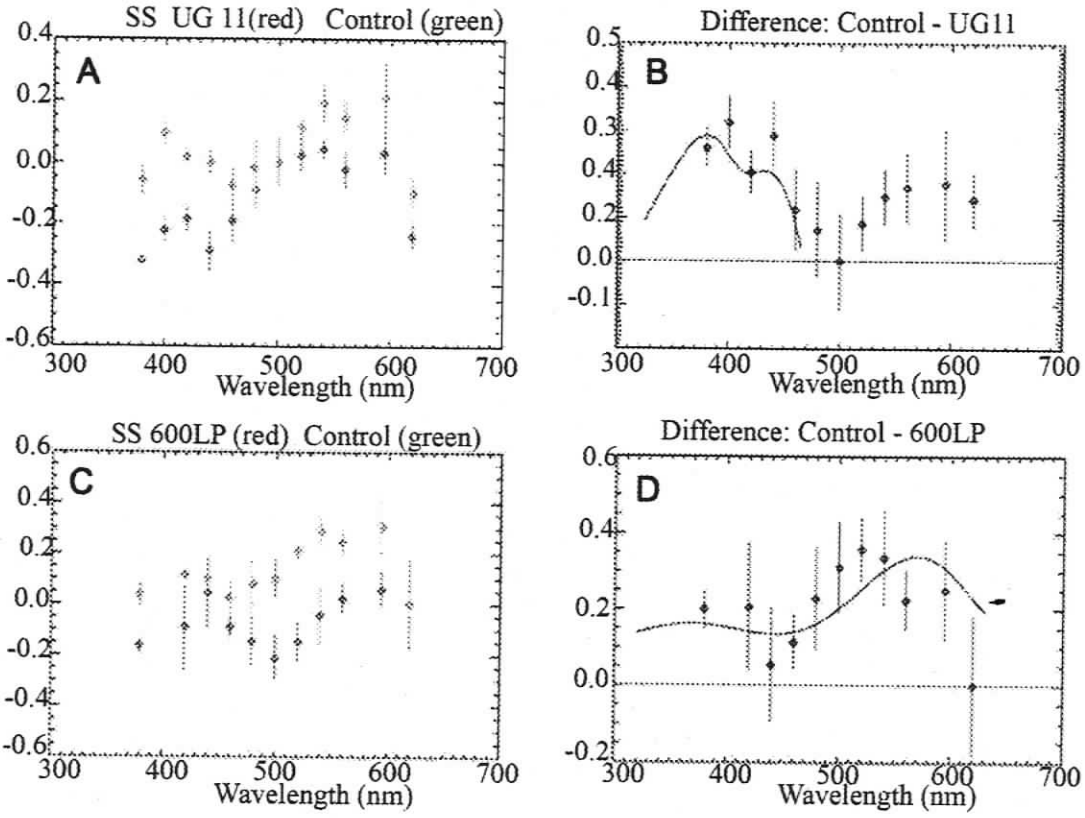

Figure 3.3 Mean normalized spectral sensitivity of rainbow trout (+/- one standard error) using ERG recording. For each treatment condition, panels on the left side show the spectral sensitivity curves for the control and treatment conditions and the panels on the right side represent the difference curves between the control and treatment spectral sensitivity. Green points represent the control and red points represent the treatment condition. The sensitivity measurements were normalized to 360 nm. A Mean normalized spectral sensitivity of: (i) control fish where the spectral sensitivity was measured using a broad-spectrum tungsten halogen background (n=3); (ii) treatment fish where spectral sensitivity was measured using a broad spectrum and UG-11 background (n=3). B Mean difference spectrum as a result of short wavelength chromatic adaptation (UG-11 filter). The black line fitted to the data points at the shortwave end of the spectrum represents an additive function based on the UVS and SWS visual pigment templates. C Mean normalized spectral sensitivity of: (i) same control fish from panel a of this figure; (ii) treatment fish where spectral sensitivity was measured using a broad spectrum and 600 nm long pass background (n=3). D Mean difference spectrum as a result of long wavelength chromatic adaptation (600 nm long pass filter). The black line fitted to the points represents the LWS cone visual pigment template.

detectable changes in cone mechanism sensitivity (demonstrated by the difference spectra in Figures 3.3 B and D) while leaving the overall modulation amplitude in polarization sensitivity relatively unchanged (i.e. less than 1 log unit difference). The solid black lines in Figures 3.3 B and D represent the cone absorption spectra of the adapted mechanisms. Note in figure 3.3 B there are two areas that exhibit sensitivity changes: one reflecting the reduced sensitivity of the UVS mechanism at the short-wavelength end of the spectrum, and a portion of the long-wavelength end where the UG-11 filter is known to have a secondary transmission band allowing a slight adaptation of the LWS mechanism.

Polarization sensitivity: ERG and CAP

Figure 3.4 shows that ERG and CAP recording techniques produce notably different polarization sensitivity curves: (i) the classic W-shaped PS curve for CAP recording (Figure 3.4B); and (ii) a four-peaked PS curve for ERG recording (Figure 3.4A). When a spectrally broad background was used for both experiments, the ERG recordings produced a sensitivity function with four maxima and four minima. This curve is similar to that described by Hawryshyn *et al.* (2003) for damselfish with maxima at 0°, 45°, 90°, 135° and 180° and minima recorded at 30°, 60°, 120° and 165°. The intermediary peaks that occurred at 45° and 135° in this study were not present in the CAP recordings made under the same background and stimulus conditions. Although a small secondary peak at 135° could also be seen in the CAP response, the secondary peaks are a prominent feature of the ERG and very minor in the CAP. Since the CAP response has been described in detail elsewhere, the rest of the paper will focus upon the ERG responses.

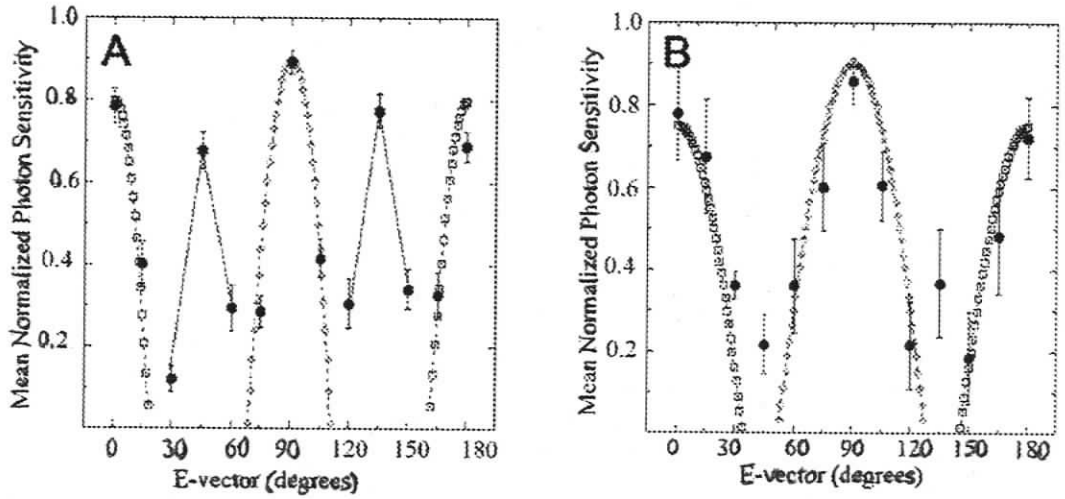

Figure 3.4. Mean ultraviolet polarization sensitivity of rainbow trout (+/- one standard error). Two different recording techniques were used, ERG and CAP recording (solid circle symbols). For Figures 4, 5, 8, the square symbols represent S_v and the diamond symbols represent S_h (see Table 2 for weighting coefficients). Dashed lines connect the symbols. A ERG PS (n=21). The solid line connects the sensitivity points representing the intermediary peaks. B CAP PS (n=5). For both figures, a 360 nm linear polarized stimulus in 15° e-vector increments was used. Note the differences in sensitivity between the two curves at 45° and 135°.

The effect of the chromatic adaptation conditions (see Spectral Sensitivity section) on polarization sensitivity was tested to assess the relative contributions of the UVS and LWS cone mechanisms to the ERG PS curve. As noted above, detection of vertically polarized light is dominated by the UVS cone mechanism whereas detection of horizontally polarized light is dominated by the LWS cone mechanism. If the intermediate peaks are due to an opponent interaction between these two polarization mechanisms, chromatic adaptation would lead to a shift of the intermediate peak away from the peak dominated by the adapted cone system. Figure 3.5A shows that when the LWS cone mechanism was adapted the intermediary peaks shifted consistently from 45° and 135°, to 60° and 120° respectively. Similarly, chromatic adaptation with UG-11 (UV Chromatic adaptation) shifts the peaks in the opposite direction, towards the vertical detector mechanism (Figure 3.5B). Therefore, the selective adaptation of either the vertical or horizontal detector led to a predictable shift of the intermediary peaks.

Cobalt chloride

In order to assess the influence of horizontal cell feedback to the cone mechanisms on spectral and polarization sensitivity, ERG experiments were conducted in conjunction with intraocular injections of cobalt chloride. Injections of concentrations of cobalt chloride higher than 0.325 mM, abolished PS as measured by b-wave amplitude (result not shown). The ERG waveforms after injection of 0.275mM Co^{2+} (Figure 3.6A) differed from the control (Figure 3.6B) in several key respects: (i) the a-wave amplitude of the cobalt treated fish was lower than the in the control; (ii) the b-wave waveform of cobalt treated fish had a temporal bandwidth significantly broader than in the control; (iii) the c-wave was absent or not apparent in cobalt treated fish; (iv) the d-wave waveform of cobalt treated fish had a temporal bandwidth significantly broader than the control.

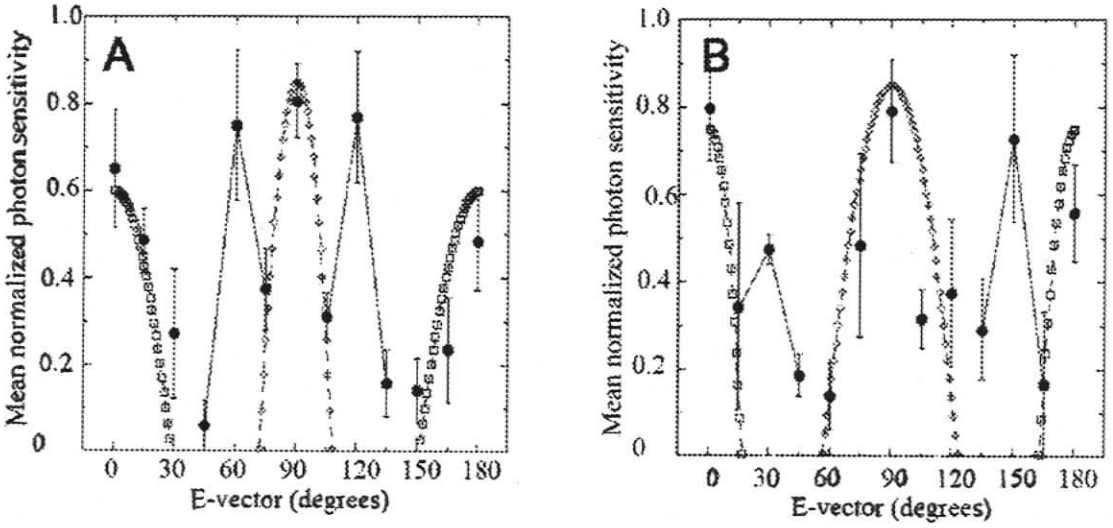

Figure 3.5 Mean ultraviolet polarization sensitivity of rainbow trout (+/- one standard error). **A** ERG UV PS with LWS cone mechanism adaptation using the 600 nm long pass background (n=3). Note the intermediary peak shifts towards the horizontal polarization mechanism and the angular breadth of the horizontal polarization mechanism decreases while the vertical polarization mechanism increases. **B** ERG UV PS with UVS cone mechanism chromatic adaptation using a UG-11 background (n=3). Note the intermediary peaks shift towards the vertical polarization mechanism and the angular breadth of the horizontal polarization mechanism increases and the vertical decreases. See Table 3.2 for linear subtractive model weighting functions.

Table 3.2 Weighting factors for computations using the linear subtractive model (equations 4&5).

Weighting Factors

Condition	k_1	k_2	k_3	k_4
CAP Figure 4A	0.75	1.6	1.5	0.9
ERG Figure 4B	0.8	7.0	6.0	0.9
600 LP adaptation Figure 5A	0.6	2.0	8.0	0.85
UG-11 adaptation Figure 5B	0.75	8.0	2.0	0.85
Cobalt Figure 8A	0.78	5.0	5.0	0.7
Saline Figure 8B	.075	1.6	1.5	0.8

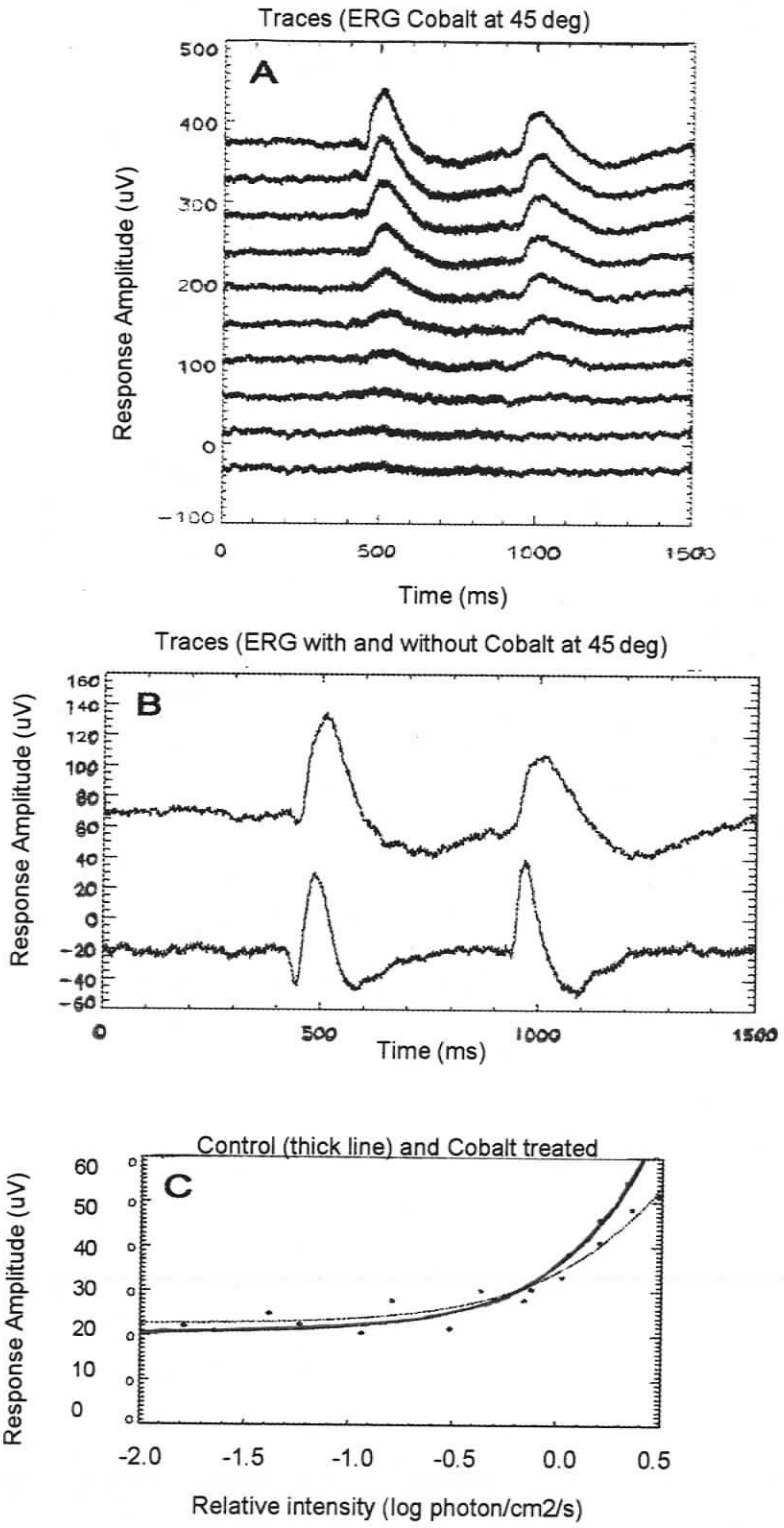

Figure 3.6 Analysis of the effect of cobalt chloride on ERG responses. A ERG waveforms at increasing intensities recorded from a cobalt treated fish (intraocular injection of cobalt chloride (intraocular concentration of 0.275 mM)). B Comparison of ERG waveforms from cobalt injected fish (upper trace) and the control (lower trace). C Response versus intensity based on ERG data taken from a cobalt chloride injected fish and a control fish. The cobalt-injected fish show a lower slope in the dynamic range resulting in a difference in the interpolated threshold intensity.

Figure 3.6C shows that these different response dynamics resulted in different threshold intensities for identical stimulus conditions and therefore different response versus intensity curves (control – black line, cobalt treated – redline), with cobalt-treated fish having a higher threshold intensity. The magnitude of difference between the two curves and hence threshold intensities varied for each individual with a range of difference between 0.2 - 0.6 log unit. Sham injections of equal amount of NaCl did not lead to significant change in response shape or sensitivity.

No significant change in spectral sensitivity was found after Co^{2+} injections (Figure 3.7A), although the difference curve (Figure 3.7B) indicates a small reduction of sensitivity in the short-wavelength end of the spectrum and slightly enhanced sensitivity to longer wavelengths.

Polarization sensitivity was significantly affected by cobalt chloride. Concentrations of 0.275mM Co^{2+} resulted in a complete collapse of the intermediate peaks (Figure 3.8A). In this condition, both the ERG and the CAP had peaks at 0°, 90°, and 180°. Sham injections (Figure 3.8B) did not change the tuning curve at all, illustrating that the intraocular injections had little influence on PS.

Discussion

Polarization vision depends on the possession of at least two differentially sensitive polarization detectors and the requisite neural network for processing receptor input. These experiments show that critically different PS tuning curves are produced depending on the recording technique used, indicating that some processing of PS occurs between the outer and inner retina and this appears to be mediated by horizontal

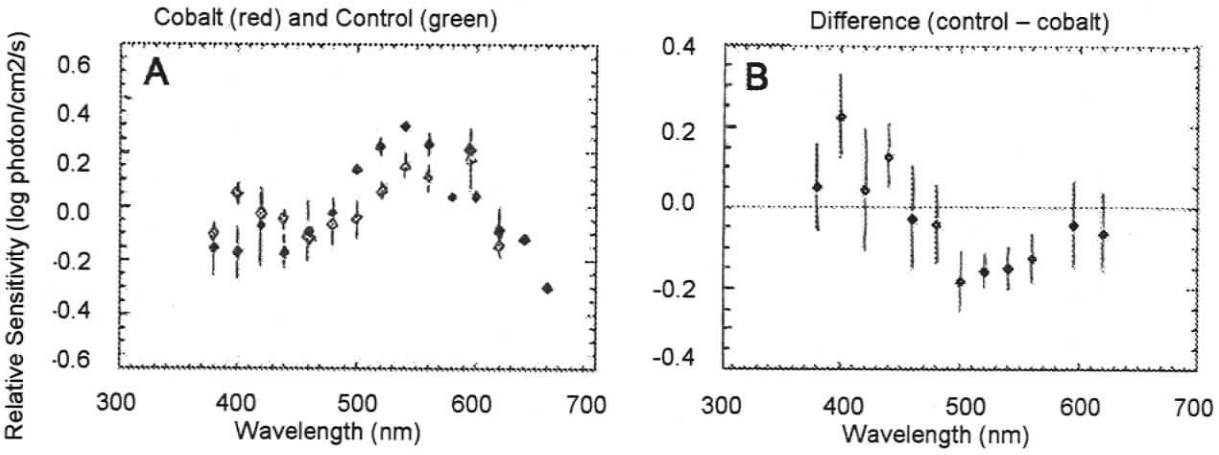

Figure 3.7 Mean normalized spectral sensitivity (+/- one standard error). A Sensitivity of control fish (n=3) in green and cobalt chloride treated fish (n=3) in red (estimated intraocular concentration was 0.275 mM). B Mean difference spectrum (control minus treated).

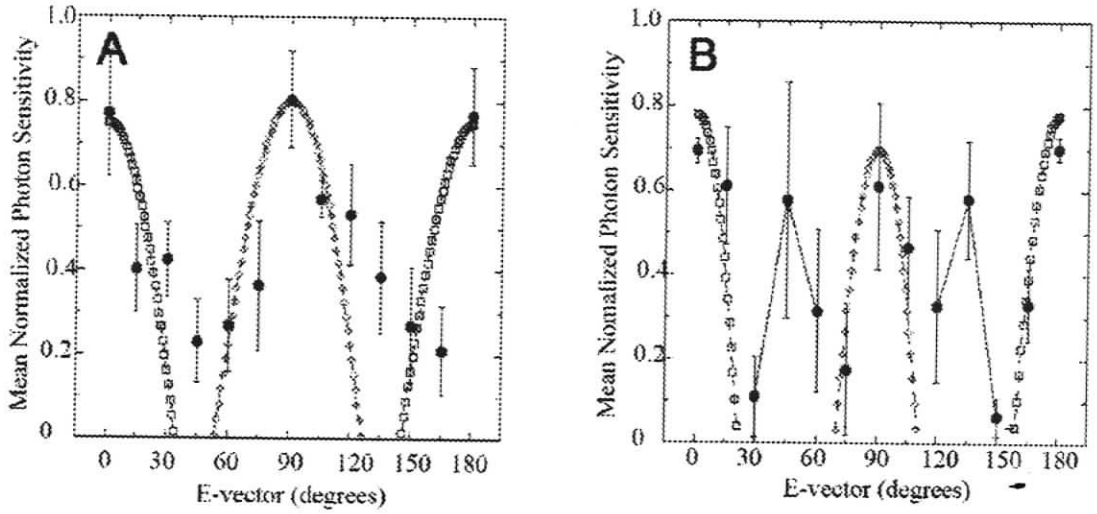

Figure 3.8 Mean ultraviolet polarization sensitivity of rainbow trout (+/- one standard error). **A** ERG UV PS of fish treated with cobalt chloride (intraocular concentration ~ 0.275 mM) (n=3). **B** Sham control intraocular injection of saline (n=3). See Table 2 for linear subtractive model weighting factors.

cells. Retinal information transfer of polarization results from network processing in both the outer and inner retina producing e-vector coding in ganglion cells (Coughlin and Hawryshyn, 1985). Here we discuss experiments and modeling of processes in the outer retina that integrate polarized light stimuli.

ERG Waveform Characteristics under Cobalt Treatment

Our study revealed significant differences in the ERG waveform characteristics of control and cobalt chloride treated test fish. For instance, the a-wave component was diminished in cobalt treated fish in relation to the control. Recent studies have shown that cobalt treatment can block inward currents in cone (Thoreson and Burkhardt, 1990) and rod (Green and Kapousta-Bruneau, 1999; Yuan and Yang, 1997) photoreceptors resulting in a suppression of signal transmission. Cobalt concentrations of 5 – 10 mM block all voltage gated calcium currents as well as calcium-dependent synaptic transmission (Thoreson and Burkhardt, 1990). Yuan and Yang (1997) suggest that cobalt-induced signal suppression results from a blockage of glutamate uptake by photoreceptors.

Sub-millimolar concentrations of cobalt are known to block horizontal cell-mediated feedback in goldfish retina (Fahrenfort *et al.,* 2004; Thoreson and Burkhardt, 1990), where connexin-mediated hemichannels are blocked. With a reduction in negative feedback the feed-forward signal would be expected to increase in amplitude but this was not evident. Rather we observed temporally broader b-wave and d-wave components, which suggests that blocking horizontal cell feedback with cobalt treatment eliminates the high pass filtering characteristic of feedback. The abnormal b-wave to a-wave ratio that results in the cobalt treated retina when compared to control is consistent with a defect in signal transmission in the outer plexiform layer (Perlman, 1983).

A recent study has shown that cobalt chloride can result in the production of hypoxia-induced factor-1alpha in retinal pigment epithelial cells (Wang *et al.,* 2005). Thus cobalt treatment can mimic hypoxic conditions in the retinal pigment epithelium, suppressing the c-wave as observed in our recordings.

HC Processing Determines Position of Intermediary PS Peaks

The responses of horizontal cells to UV stimuli remain largely uncharacterized (fish retina – Nakano *et al.,* 2006; Fukurotani and Hashimoto, 1984; Hashimoto *et al.,* 1988, and turtle retina - Ammemuller *et al.*, 1998; Ventura *et al.*, 1999; Ventura *et al.*, 2001; Zana *et al.*, 2001), despite the wealth of research directed at the role of horizontal cells in colour processing. Moreover, there are no data examining the response of horizontal cells to linearly polarized light. The search for UV polarization–sensitive horizontal cells represents an immediate concern for those working on polarization vision in vertebrates.

Kamermans and coworkers have assessed important features of the spectral characteristics of the feedback signals, derived from horizontal cells, in goldfish cones. Kraaij et al. (1998) showed that the feedback signals measured in the LWS, MWS and SWS cones were spectrally very broad and never reversed in polarity. In addition, the feedback signals peaked near (in the case of the LWS cone) or at longer wavelengths (for the MWS and SWS cones) than the peak absorbance for the cone class itself.

Cone synaptic gain strongly depends on the strength of feedback received from horizontal cells, which makes the synaptic gain of the cones strongly dependent on the spectral composition of the surround (Verweij *et al.,* 1996). A full-field stimulus used to stimulate one photoreceptor type near its λ_{max} will produce hyperpolarization in that cone type and inhibitory feedback to all cone classes, which has a relatively larger depolarizing effect on other cone classes (Kamermans *et al.,* 1998). The strength of the

signals passed onto the bipolar cell network from the various cone classes (i.e., the feed-forward signal) can therefore be affected by altering the spectral distribution and intensity of the background and stimulus conditions. In addition, studies on turtle retina have shown that cone – cone coupling can lead to the LWS cone mechanism providing excitatory input to SWS cone mechanism (Itzhaki *et al.,* 1992). Cone – cone coupling could enhance sensitivity if two differentially sensitive photoreceptor mechanisms were stimulated in a zone of overlapping sensitivity (spectral or polarization).

Our experiments targeted manipulation of the first neural stages involved in the detection and processing of polarized light. Shifts in the location of the intermediary peaks under differing chromatic conditions may be explained by relative changes in the strength of HC feedback among the cone classes. If the feedback signal from the horizontal cell network to UVS cone mechanism shares the same spectral response characteristics as that seen in other cone types (Kraaij *et al.,* 1998), the full-field UV stimulus used in these experiments on a spectrally broad background would generate a relatively larger inhibitory feedback effect on the LWS mechanism than on the UVS mechanism. These photic conditions produced relatively balanced signals from both the horizontal and vertical mechanisms as measured by b-wave amplitude and result in the symmetrical four-peaked polarization-tuning curve (Figures 3.4A). Chromatic adaptation using long-wavelength adaptation condition reduces the hyperpolarization or feed-forward response of the LWS cones/horizontal channel and reduces inhibitory feedback in the UVS cones. This results in a relatively larger contribution from the vertical channel, as seen by the shift in the location of the intermediary peaks from 45° and 135° degrees to 60° and 120° degrees (Figure 3.5B). Similarly, chromatic adaptation of the UVS cone mechanism would reduce the hyperpolarization responses of the UVS cones, reducing both the feed-forward signal from the vertical channel and the inhibitory feedback on the

horizontal channel, resulting in a relative increase of the LWS/horizontal channel feed-forward signals (Fig. 3.5B). This expansion of the horizontal channel is consistent with the narrowing of the UVS mechanism seen in the shifting of the intermediary peaks from their original location at 45° and 135° degrees to 30° and 150° (Figure 5b). In both the UVS and LWS cone mechanism adaptation conditions, we successfully demonstrated that PS results from differential sensitivity in cone mechanisms, and when the contributions of these cone mechanisms were altered, so too was the interaction between the PS mechanisms. The observed angular shifts argue strongly for the presence of opponent interactions between the vertical and horizontal detector mechanisms. Manipulation of the sensitivity of the polarization detectors produces predictable displacement of the intermediary peaks and bandwidth of polarization detector mechanisms.

Intermediary peaks are generated by HC feedback and inhibited by cobalt

Previous studies have demonstrated that sub-millimolar concentrations of cobalt inhibit feedback-induced responses in cones (Fahrenfort *et al.,* 2004; Thoreson and Burkhardt, 1990) and selectively inhibit the surround responses in bipolar cells without attenuating the central ON or OFF bipolar signal (Vigh and Witkovsky, 1999). Intraocular concentrations of 0.275 mM cobalt reduced HC feedback and eliminated the intermediary peaks (compare Figures 3.8a and 3.8b). This suggests that the intermediary peaks are a function of feedback activity, and that a significant reduction in HC feedback results in the two channels being expressed primarily in the feed-forward pathways. To support the hypothesis that the intermediary peaks are the result of feedback, we need to identify a feed-forward signal that generates the ON-bipolar response and which is reduced when feedback is reduced. Our results suggest that such a reduction in feed-forward signals occurs in both the chromatic adaptation conditions

and the cobalt treatments. During the UVS cone adaptation and cobalt treatments, there is a relative reduction in the UVS cone mechanism feed-forward signal due to the reduction in feedback onto the LWS/horizontal mechanism. The LWS cone mechanism adaptation condition produces a relative reduction in inhibitory feedback onto the UVS cones, resulting in a relatively smaller feed-forward signal from the LWS/horizontal mechanism compared to the other conditions.

Interneuronal processing of PS

The results of this study show that the two electrophysiological techniques (CAP and ERG) produce significantly different PS curves and that those differences are likely the result of interneuronal processing mediated by horizontal cells. For instance, cobalt treatment is known to eliminate horizontal cell feedback onto cones and suppresses the intermediary peaks present in ERG recordings. The disappearance of intermediary peaks under cobalt treatment may indicate the removal of an element of network processing involved in the integration of distinct processing modules that monitor physical attributes of the polarization stimulus, such as intensity and percent polarization. Polarization sensitivity becomes functional when both the intensity and percent polarization of the stimulus fall within a critical dynamic range. A diminished contribution of these parameters compromises the ability of the outer retina to produce a signal of sufficient magnitude to enable e-vector encoding. This prediction is supported by empirical data that show percent polarization and intensity represent critical determinants of polarization sensitivity. When intensity (Hawryshyn, 1991; Parkyn and Hawryshyn, 1993) and percent polarization (Hawryshyn and Bolger, 1990; Parkyn and Hawryshyn, 2003; Novales Flamarique and Hawryshyn, 1997) fall within the critical range for operation of the polarization network, bipolar cells provide input to the inner retina. We propose that the inner retina provides another level of network processing

that operates to code e-vector. Single-unit recordings from the optic nerve (Hawryshyn, unpublished) and ganglion cell axon terminations in the *torus semicircularis* (Coughlin and Hawryshyn, 1995) exhibit opponent responses to linearly polarized light. Furthermore, UV PS curves recorded from ganglion cell terminations in the *torus semicircularis* are W-shaped and coded on the basis of e-vector (e.g. ON for vertical, OFF for horizontal). Thus we propose polarization information transfer occurs through levels of network processing where first, all relevant physical attributes of the polarized stimulus are assessed in the outer retina and subsequently, e-vector is encoded at the level of a second network, very likely, the inner retina.

In a related study, *Chromis viridis*, a species that has an ERG polarization sensitivity tuning curve similar to that seen in rainbow trout (Hawryshun et al., 2003), was capable of selecting and behaviourally discriminating between the horizontal and vertical plane of UV linearly polarized light independent of the stimuli brightness content (Mussi et al., 2006). The capacity for e-vector discrimination disappeared when the UV portion of the light stimuli was removed indicating that the presence of UV polarized light is critical for e-vector discrimination. In addition, fish were able to distinguish between relatively small differences in e-vector orientation, with the minimum separable e-vector discrimination in comparison with the reference e-vector between 15°-25°. The discriminative performance of *C. viridis* was greatest at e-vector orientations where the two polarization detector mechanisms have overlapping sensitivity. Thus polarization discrimination appears to be at its optimal level of performance when the two detector mechanisms are interacting through interneuronal processing mediated by horizontal cells.

Electrophysiological and pharmacological assessment of the processing of polarized light in the retina (Chapter 3) suggests that horizontal cells play a substantial role in mediating polarization sensitivity in teleosts. This research provides the first evidence of neural processing of PS in the OPL of the retina and demonstrates that critically different polarization sensitivity tuning curves are produced depending on the recording technique used. The finding that HCs have a specialized contribution in the processing of polarized light is consistent with a model being developed by the Hawryshyn lab which proposes that the strength of feed-forward (cone input) and feedback signals coding horizontal and vertical e-vector to different classes of HCs form the basis of e-vector coding in the HC network. Our experiments provide evidence that HC processing accentuates opponency between the photoreceptors that exhibit orthogonal e-vector sensitivity, and this opponent interaction is expected to form the basis of e-vector coding demonstrated by higher order neurons in the CNS. However, these results do not answer the question of whether there are different classes of HCs with respect to e-vector coding, namely whether different layers of horizontal cells will exhibit differential responses to vertical and horizontal planes of polarized light.

Although there have been no assessments of the responses of retinal interneurons to plane polarized light, recent work (Nakano *et al.,* 2006) has provided the first description of the responses of HCs in a salmonid to UV light. Working with masu salmon, Nakano *et al.* (2006) identified six types of HCs (three luminosity types and three chromaticity types), all of which exhibited relatively large-amplitude hyperpolarizing responses to UV stimuli, thereby suggesting a different pattern of HC processing in the UV portion of the spectrum than for wavelengths between 400 and 700nm. However, in contrast to earlier work examining HC responses to UV light in cyprinids (Fukurotani & Hashimoto, 1984, Harosi and Fukurotani, 1986; Hashimoto *et al.*, 1988), Nakano *et al.*

(2006) did not find evidence of tetraphasic HCs. Additional experimental data concerning the spectral and polarization sensitivity of HC responses and feedback to cone photoreceptors are required in order to accurately characterize roles of HCs and contribute to models of connectivity and function.

The protocols and experimental results obtained using the WPC technique to assess spectral sensitivity (Chapter 2) lay the necessary groundwork to use WPC to further elucidate the signaling pathway between HCs and cone photoreceptors. The WPC technique may not be optimal for the assessment of spectral sensitivity, given the slower rate of data collection compared to techniques such as MSP. However, in addition to measuring sensitivity at longer wavelengths and lower values of absolute sensitivity than are accessible by spectrophotometry, it is a technique which affords the opportunity to assess cell signaling characteristics in an intact neural network that are not available through other means. For example, WPC can be used to assess the UV-stimulus generated feedback signals from HCs to all classes of cone photoreceptors. Based on our findings that HCs play a key role in modulating UV-based PS, as well as the recent research examining HC responses to UV light described above (Nakano *et al.,* 2006), I expect the responses to UV stimuli will generate a distinct component of the spectral sensitivity curve describing HC feedback. WPC can also be used to investigate the specific ionic currents involved in generating the feedback currents. Of particular interest would be an assessment of the calcium current in cones, which is known to be modulated by HC feedback (Verweij *et al.,* 1996), and the relative changes in signaling which occur when this current is blocked through the addition of cobalt chloride to the perfusate (see Barnes and Hille, 1989).

Although Palacios *et al.* (1998b) published measures of dichroic absorption of dissociated amphibian rods, based on differential sensitivity to orthogonally polarized UV light stimuli using a suction pipette electrode, to date there have been no attempts to

assess polarization sensitivity in cone photoreceptors using WPC or other intracellular techniques. While the neural connections in the retina remain intact in the tissue preparation used for WPC, the geometry of the cone mosaic most likely does not. An assessment of whether cone photoreceptor or HC feedback signals exhibit polarization sensitivity using WPC would therefore also have implications for the biophysical models underlying PS.

Aidley DJ (1998) The Physiology of Excitable Cells, 4th edn. Edition: Cambridge University Press.

Alexander G, Sweeting R, McKeown B (1994) The shift in visual pigment dominance in the retinae of juvenile coho salmon (*Oncorhynchus kisutch*): an indicator of smolt status. *Journal of Experimental Biology* 195:185-197.

Allen DM, Munz FW (1983) Visual pigment mixtures and scotopic spectral sensitivity in rainbow trout. *Environ Biol Fishes* 8:185-190.

Allen DM, Loew ER, McFarland WN (1982) Seasonal change in the amount of visual pigment in the retinae of fish. *Canadian Journal of Zoology* 60:281-287.

Allen DM, McFarland WN, Munz FW, Poston HA (1973) Changes in the visual pigments of trout. *Canadian Journal of Zoology* 51:901-914.

Allison WT, Dann SG, Veldhoen KM, Hawryshyn CW (2006) Degeneration and regeneration of ultraviolet cone photoreceptors during development in rainbow trout. *Journal of Comparative Neurology* 499:702-715.

Allison WT, Dann SG, Helvik JV, Bradley C, Moyer HD, Hawryshyn CW (2003) Ontogeny of ultraviolet-sensitive cones in the retina of rainbow trout. *Journal of Comparative Neurology* 461:294-306.

Ammemuller, J., Itzhaki, A., Weiler, R. and Perlman, I. (1998). UV-sensitive input to horizontal cells in the turtle retina. *European Journal of Neuroscience* 10: 1544-1552.

Avery JA, Bowmaker JK, Djamgoz MBA, Downing JEG (1983) Ultra-violet photoreceptors in a freshwater fish. *Journal of Physiology* 334:23P-24P.

Barnes, S. and Hille, B. (1989) Ionic channels of the inner segment of tiger salamander cone photoreceptors. *Journal of General Physiology* 94 (4) 719-743.

Barry, K. L. and Hawryshyn, C. W. (1999). Spectral sensitivity of the Hawaiian saddle wrasse, *Thalassoma duperrey*, and implications for visually mediated behaviour on coral reefs. *Environmental Biology of Fishes* 56: 429-442.

Baylor DA, Nunn BJ, Schnapf JL (1987) Spectral sensitivity of cones of the monkey *Macaca fascicularis*. *Journal of Physiology* 390:145-160.

Baylor, D. A., Fuortes, M. G. F. and O'Bryan, P. M. (1971). Receptive fields of cones in the retina of the turtle. *Journal of Physiology* 214: 265-294.

Beatty DD (1966) A study of the succession of visual pigments in Pacific salmon (Oncorhynchus). *Canadian Journal of Zoology* 44:429-455.

Beaudet L, Browman HI, Hawryshyn CW (1993) Optic Nerve Response and Retinal Structure in Rainbow Trout of Different Sizes. *Vision Research* 33:1739-1746.

Bennett ATD, Cuthill IC (1994) Ultraviolet vision in birds: what is its function? *Vision Research* 34:1471-1478.

Bernard, G.D., Wehner, R. (1977) Functional similarities between polarization vision and colour vision. *Vision Research* 17: 1019-1028

Bilotta J, Saszik S. 2001. The zebrafish as a model visual system. *International Journal of Developmental Neuroscience* 19: 621–629

Bowmaker JK (1995) The visual pigments of fish. *Progress in Retinal and Eye Research* 15:1-31.

Bowmaker JK (1998) Evolution of colour vision in vertebrates. *Eye* 12:541-547.

Bowmaker JK, Kunz YW (1987) Ultraviolet receptors, tetrachromatic colour vision and retinal mosaics in the brown trout (*Salmo trutta*): age-dependent changes. *Vision Research* 27:2101-2108.

Bowmaker JK, Hunt DM (1999) Molecular biology of photoreceptor spectral sensitivity. In: Adaptive Mechanisms in the Ecology of Vision (Archer SN, ed), pp 439-462. Kluwer: Dordrechct.

Bridges CDB (1965) The grouping of fish visual pigments about preferred positions in the spectrum. *Vision Research* 5:223-238.

Bridges CDB (1967) Spectroscopic properties of porphyropsins. *Vision Research* 7:349-369.

Browman HI, Hawryshyn CW (1994) The developmental trajectory of ultraviolet photosensitivity in rainbow trout is altered by thyroxine. *Vision Research* 34:1397-1406.

Brown, K. T. (1968). The electroretinogram: its components and their origin. Vision Research 8: 633-677

Brown PK, Gibbons IR, Wald G (1963) The visual cells and visual pigment of the mudpuppy, *Nectarus*. *Journal of Cell Biology* 19:79-106.

Burkhardt, D.A. (1993) Synaptic feedback, depolarization and color opponency in cone photoreceptors. *Visual Neuroscience* 10: 981-989

Burkhardt DA (1989) The spectral sensitivity of a passerine bird is highest in the UV. *Naturwissenschaften* 76:82-83.

Cheng A, Novales Flamarique I, Harosi FI, Rickers-Haunerland J, Haunerland NH (2006) Photoreceptor layer loss of salmonid fishes: transformation and loss of single cones in juvenile fish. *Journal of Comparative Neurology* 495:213-235.

Chrachi A, Nelson L, Willisamson R (2005) Whole-cell recording of light-evoked photoreceptor responses in a slice preparation of the cuttlefish retina. *Visual Neuroscience* 22:359-370.

Coughlin, D. J. and Hawryshyn, C. W. (1995). A Cellular Basis for Polarized-Light Vision in Rainbow-Trout. *Journal of Comparative Physiology A* 176: 261-272.

Coughlin DJ, Hawryshyn CW (1994a) The contribution of ultraviolet and short-wavelength sensitive cone mechanisms to color vision in rainbow trout. *Brain Behaviour Evolution* 43:219-232.

Coughlin DJ, Hawryshyn CW (1994b) Ultraviolet sensitivity in the torus semicircularis of juvenile rainbow trout *(Oncorhynchus mykiss)*. *Vision Research* 34:1407-1413.

Cronin, T. W. and Shashar, N. (2001). The linearly polarized light field in clear, tropical marine waters: Spatial and temporal variation of light intensity, degree of polarization and e-vector angle. *Journal of Experimental Biology* 204: 2461-2467.

Dann SG, Allison WT, Levin DB, Hawryshyn CW (2003) Identification of a unique transcript down-regulated in the retina of rainbow trout (*Oncorhynchus mykiss*) at smoltification. *Comparative Biochemistry and Physiology B-Biochemistry & Molecular Biology* 136:849-860.

Dartnall HJA (1953) The interpretation of spectral sensitivity curves. *British Medical Bulletin* 9:24-30.

Dartnall HJA, Lythgoe JN (1965) The spectral clustering of visual pigments. *Vision Research* 5:81-100.

Daumer K (1956) Reizmetrische Untersuchung des Farbensehens der Bienen. *Zeitschrift fur vergleichende Physiologie* 38:413-478.

Degner, S. & C.W. Hawryshyn. 2001. Orientation of rainbow trout (*Oncorhynchus mykiss*) to linearly polarised light fields. *Canadian Journal of Zoology* 79: 407-415

DeMarco, P.J., Jr., and Powers, M.K. (1989). Sensitivity of ERG components from dark-adapted goldfish retinas treated with APB. *Brain Research* 482:317-23.

Douglas RH, McGuigan CM (1989) The spectral transmission of freshwater teleost ocular media - an interspecific comparison and a guide to potential ultraviolet sensitivity. *Vision Research* 29:871-879.

Dowling JE, Ehinger B (1978) The interplexiform cell system. I. Synapses of the dopaminergic neurons of the goldfish retina. *Proc R Soc Lond* [Biol] 201:7-26.

Fahrenfort, I., Sjoerdsma, T., Ripps, H. and Kamermans, M. (2004). Cobalt ions inhibit negative feedback in the outer retina by blocking hemichannels on horizontal cells. *Visual Neuroscience* 21:501-511.

Fineran, B. A. and Nicol, J. A. C. (1978). Studies on Photoreceptors of *Anchoa mitchilli* and *Anchoa hepsetus* (Engraulidae) with Particular Reference to Cones. *Phil Trans Roy Soc London Series B-Biological Sciences* 283: 25-60.

Firsov ML, Govardovskii VI, Donner K (1994) Response univariance in bull-frog rods with two visual pigments. *Vision Research* 34:839-847.

Fukurotani, K., Hashimoto, Y (1984) A new type of S-potential in the retina in cyprinid fish: the tetraphasic spectral response. *IOVS* (Suppl): 24, 118

Fuortes MGF, Simon EJ (1974) Interactions leading to horizontal cell responses in the turtle retina. *Journal of Physiology* 240:177-198.

Gal, J., Horvath, G., Barta, A. S. and Wehner, R. D. (2001). Polarization of the moonlit clear night sky measured by full-sky imaging polarimetry at full Moon: Comparison of the polarization of moonlit and sunlit skies. *J Geophys Res Atmosp* 106: 22647-22653.

Gouras P (2006) Colour Vision. In. Webvision: Kolb, H, Fernandez, E. & Nelson, R.

Govardovskii VI, Fyhrquist N, Reuter T, Kuzmin DG, Donner K (2000) In search of the visual pigment template. *Visual Neuroscience* 17:509-528.

Green, D.G., Kapousta-Bruneau, N.V. (1999) A dissection of the electroretinogram from isolated rat retina with microelectrodes and drugs. *Visual Neuroscience* 16: 727-741

Guthrie DM (1990) The physiology of the teleostan optic tectum. In: The Visual System of Fish (Douglas RH, Djamgoz MBA, eds). London: Chapman and Hall.

Harosi FI (1985) Ultraviolet and violet absorbing vertebrate visual pigments: Dichrotic and bleaching properties. In: The visual system (Fein A, Levine J, eds), pp 41-55. New York: Liss.

Harosi FI (1994) An analysis of two spectral properties of vertebrate visual pigments. *Vision Research* 34:1359-1367.

Harosi FI, Hashimoto Y (1983) Ultraviolet visual pigment in a vertebrate: A tetrachromatic cone system in the dace. *Science* 222:1021-1023.

Hashimoto Y, Harosi FI, Ueki K, Fukurotani K-K (1988) Ultra-violet sensitive cones in the color-coding systems of cyprinid retinas. *Neuroscience Research* Suppl. 8:S81-S95.

Hawryshyn, C.W. (1991) Light adaptation properties of the ultraviolet-sensitive cone mechanism in comparison to the other receptor mechanisms of goldfish. *Visual Neuroscience* 6: 293-301.

Hawryshyn CW (1992) Polarization vision in fish. *American Scientist* 80:164-175.

Hawryshyn CW (2000) Ultraviolet polarization vision in fishes: possible mechanisms for coding e-vector. *Phil Trans Roy Soc London Series B-Biological Sciences* 355: 1187-1190.

Hawryshyn, C. W., Arnold, M. G., Bowering, E. and Cole, R. L. (1990). Spatial Orientation of Rainbow-Trout to Plane-Polarized Light - the Ontogeny of E-Vector Discrimination and Spectral Sensitivity Characteristics. *Journal of Comparative Physiology A* 166: 565-574.

Hawryshyn CW, Beauchamp R (1985) Ultraviolet photosensitivity in goldfish: an independent UV retinal mechanism. *Vision Research* 25:11-20.

Hawryshyn CW, McFarland WN (1987) Cone photoreceptor mechanisms and the detection of polarized light in fish. *Journal of Comparative Physiology A* 160:459-465.

Hawryshyn CW, Harosi FI (1994) Spectral characteristics of visual pigments in rainbow trout (*Oncorhynchus mykiss*). *Vision Research* 34:1385-1392.

Hawryshyn CW, Haimberger TJ, Deutschlander ME (2001) Microspectrophotometric measurements of vertebrate photoreceptors using CCD-based detection technology. *Journal of Experimental Biology* 204:2431-2438.

Hawryshyn CW, Moyer HD, Allison WT, Haimberger TJ, McFarland WN (2003) Multidimensional polarization sensitivity in damselfishes. *Journal of Comparative Physiology A* 189:213-220.

Hawryshyn CW, Martens G, Allison WT, Anholt BR (2003) Regeneration of ultraviolet-sensitive cones in the retinal cone mosaic of thyroxin-challenged post-juvenile rainbow trout (Oncorhynchus mykiss). *Journal of Experimental Biology* 206:2665-2673.

Helmholtz Hv (1896) Handbuch der physiologischen Optik, 2nd ed Edition. Hamburg: Voss.

Helverson Ov (1972) Zur spektralen Unterschiedsemp-findlichkeit der Honigbiene. *Journal of Comparative Physiology* 80:439-472.

Hering E (1878) Zur Lehre vom Lichtsinne. Wien: Carl Gerold's Sohn.

Hisatomi O, Kayada S, Aoki Y, Iwasa T, Tokunaga F (1994) Phylogenetic relationships among vertebrate visual pigments. *Vision Research* 34:3097 - 3102.

Itzaki, I., Malik, S. and Perman, I. (1992) Spectral properties of short-wavelength (blue) cones in the turtle retina. *Visual Neuroscience* 9: 235-241.

Jacobs GH (1982) Comparative colour vision. New York: Academic Press.

Jacobs GH (1992) Ultraviolet vision in vertebrates. American Zoologist 32:544-554.

Joly, D. W., Mawdesley-Thomas, L. E. and Bucke, D. (1972) Anaesthesia of fish. *Vet Record* 91 424-426.

Kamermans M, van Dijk BW, Spekreijse H (1991) Color opponency in cone-driven horizontal cells in carp retina. Aspecific pathways between cones and horizontal cells. *Journal of General Physiology* 97:819-843.

Kamermans M, Kraaij DA, Spekreijse H (1998) The cone/horizontal cell network: a possible site for color constancy. *Visual Neuroscience* 15:787-797.

Kamermans M, Kraaij D, Spekreijse H (2001) The dynamic characteristics of the feedback signal from horizontal cells to cones in the goldfish retina. *Journal of Physiology* 534:489-500.

Kaneko A (1970) Physiological and morphological identification of horizontal, bipolar and amacrine cells in goldfish retina. *Journal of Physiology (London)* 207:623-633.

Kaneko A (1973) Receptive Field Organization of Bipolar and Amacrine Cells in Goldfish Retina. *Journal of Physiology-London* 235:133-153.

Kraaij DA, Kamermans M (2000) The nature of surround-induced depolarizing responses in goldfish cones. *Journal of General Physiology* 115:3-15.

Kraaij DA, Kamermans M, Spekreijse H (1998) Spectral sensitivity of the feedback signal from horizontal cells to cones in goldfish retina. *Visual Neuroscience* 15:799-808.

Kraaij DA, Spekreijse H, Kamermans M (2000) The open- and closed-loop gain-characteristics of the cone/horizontal cell synapse in goldfish retina. *Journal of Neurophysiology* 84:1256-1265.

Levine J, MacNichol EF (1982) Colour vision in fish. In: The Mind's Eye (Wolfe, J.M., ed), p Chapter 1. New York: WH Freeman.

Liebman PA, Entine G (1968) Visual pigments of frog and tadpole (Rana pipiens). *Vision Research* 8:761-775.

Loew ER, Dartnall HJA (1976) Vitamin A1/A2-based visual pigment mixtures in cones of the rudd. *Vision Research* 16:891-896.

Loew ER, McFarland WN (1990) The underwater visual environment. In: The Visual System of Fish (Douglas RH, Djamgoz MBA, eds), pp 1-43. New York: Chapman & Hall.

Loew ER, McFarland WN, E. M, Hunter D (1993) A chromatic action spectrum for planktonic predation by juvenile yellow perch, *Perca flavenscens*. *Canadian Journal of Zoology* 71:384-386.

Losey GS, Cronin TW, Goldsmith TH, Hyde D, Marshall NJ, McFarland WN (1999) The UV visual world of fishes: a review. *Journal of Fish Biology* 54:921-943.

Lythgoe JN (1988) Light and vision in the aquatic environment. In: Sensory Biology of Aquatic Animals (Atema J, Fay R, Popper A, Tavolga W, eds), p Chapter 3. New York: Springer-Verlag.

Makino CL, Dodd RL (1996) Multiple visual pigments in a photoreceptor of the salamander retina. *Journal of General Physiology* 108:27-34.

Maxwell JC (1860) On the theory of compound colours and the relations of the colours of the spectrum. Philosophical Transactions of the Royal Society of London B 150:57-84.

McFarland WN, Allen DM (1977) The effect of extrinsic factors on two distinctive rhodopsin-porphyropsin systems. *Canadian Journal of Zoology* 55:1000-1009.

McFarland, W. and Munz, F. W. (1975a). Part 2: The photic environment of clear tropical seas during the day. *Vision Research* 15: 1063-1070.

McFarland, W. and Munz, F. W. (1975b). Part III: The evolution of photopic visual pigments in fishes. *Vision Research* 15: 1071-1080.

Meek HJ (1990) Tectal morphology: connections, neurons and synapses. In: The Visual System of Fish (Douglas RH, Djamgoz MBA, eds). London: Chapman and Hall.

Miller JL, Korenbrot JI (1993) Phototransduction and adaptation in rods, single cones, and twin cones of the striped bass retina: A comparative study. *Visual Neuroscience* 10:653-667.

Munz FW, Beatty DD (1965) A critical analysis of the visual pigments of salmon and trout. *Vision Research* 5:1-17.

Mussi M., Haimberger T.J., Hawryshyn C.W. (2005) Behavioural discrimination of polarized light in the damselfish *Chromis viridis* (family *Pomacentridae*). *Journal of Experimental Biology* 208:3037-3046.

Naka NI, Rushton WAH (1966) S-potentials from colour units in the retina of fish (Cyprinidae). *Journal of Physiology* 185:536-555.

Nakano, N., Kawabe, R., Yamashita, N., Hiraishi, T., Yamamoto, K., Nasimoto, K. (2006) Color vision, spectral sensitivity, accommodation, and visual acuity in juvenile masu salmon *Oncorhynchus masou masou*. *Fisheries Science* 72: 239-249

Nave CR (2006) Hyperphysics. In. World Wide Web: Georgia State University.

Neumeyer C (1992) Tetrachromatic color vision in goldfish: evidence from colour mixing experiments. *Journal of Comparative Physiology* A 171:639-649.

Novales Flamarique, I., and Hawryshyn, C. W. (1993). Spectral Characteristics of Salmonid Migratory Routes from Southern Vancouver-Island (British-Columbia). *Canadian Journal of Fisheries and Aquatic Science* 50: 1706-1716.

Novales Flamarique, I. & C.W. Hawryshyn. (1997). Is vertebrate use of under-water polarized light restricted to crepuscular time periods? Vision Res. 37: 975-989.

Novales Flamarique, I., Hawryshyn, C. W. and Harosi, F. I. (1998). Double-cone internal reflection as a basis for polarization detection in fish. *Journal of the Optical Society of America A*. 15: 349-358.

Novales Flamarique I, Hawryshyn CW (1998) Double cone internal reflection as a basis for polarized light detection. *Journal of Optical Society of America* 15:349-358.

O'Bryan PM (1973) Properties of the depolarizing synaptic potential evoked by peripheral illumination in cones of the turtle retina. *Journal of Physiology* 235:207-223.

Palacios AG, Goldsmith TH (1993) Photocurrents in retinal rods of pigeons (Columba livia): Kinetics and spectral sensitivity. *Journal of Physiology* 471:817-829.

Palacios AG, Goldsmith TH, Bernard GD (1996) Sensitivity of cones from a cyprinid fish (*Danio aequipinnatus*) to ultraviolet and visible light. *Visual Neuroscience* 13:411-421.

Palacios AG, Varela FJ, Srivastava R, Goldsmith TH (1998) Spectral sensitivity of cones in the goldfish, *Carassius auratus*. *Vision Research* 38:2135-2146

Palacios AG, Srivastava, R., Goldsmith, TH (1998b) Spectral and polarization sensitivity of photocurrents of amphibian rods in the visible and ultraviolet. *Visual Neuroscience* 15:319-331

Pang J-J, Gao F, Wu SM (2002) Segregation and integration of visual channels: Layer-by-layer computation of on-off signals by amacrine cell dendrites. *Journal of Neuroscience* 22:4693-4701.

Parkyn DC, Austin JD, Hawryshyn CW (2003) Acquisition of polarized-light orientation in salmonids under laboratory conditions. *Animal Behaviour* 65:893-904.

Parkyn, D. C. and Hawryshyn, C. W. (1993). Polarized-light sensitivity in rainbow trout (Oncorhynchus mykiss): characterization from multi-unit responses in the optic nerve. *Journal of Comparative Physiology A* 172: 473-500.

Parkyn DC, Hawryshyn CW (2000) Spectral and polarization sensitivity of salmonids: a comparative analysis using electrophysiology. *Journal of Experimental Biology* 203:1173-1191.

Parry JW, Bowmaker JK (2000) Visual pigment reconstitution in intact goldfish retina using synthetic retinaldehyde isomers. *Vision* 40:2241-2247.

Pasino E, Marchiafava PL (1976) Transfer Properties of Rod and Cone Cells in Retina of Tiger Salamander. *Vision Research* 16:381-386.

Perlman, I. (1983). Relationship between the amplitudes of the b wave and the a wave as a useful index for evaluating the electroretinogram. *British Journal of Ophthalmology* 67, 443-448.

Piccolino M (1995) Cross-talk between cones and horizontal cells through the feedback circuit. In: Neurobiology and Clinical Aspects of the Outer Retina (Djamgoz MBA, Archer SN, Vallerga S, eds), pp 221-248. London: Chapman & Hall.

Pomozi, I., Horvath, G. and Wehner, R. (2001). How the clear-sky angle of polarization pattern continues underneath clouds: full sky measurements and implications for animal orientation. *Journal of Experimental Biology* 204: 2933-2942.

Roberts NW, Gleeson HE, Temple SE, Haimberger TJ, Hawryshyn CW (2004) Differences in the optical properties of vertebrate photoreceptor classes leading to axial polarization sensitivity. *Journal of the Optical Society of America A* 21:335-345.

Schellart NAM, Rikkert WEI (1989) Response features of the visual units in the lower midbrain of the rainbow trout. *Journal of Experimental Biology* 144:357-375.

Shashar N, Cronin TW (1996) Polarization contrast vision in Octopus. *Journal of Experimental Biology* 199:999-1004.

Shashar N, Hanlon RT (1997) Squids (*Loligo pealei* and *Euprymna scolopes*) can exhibit polarized light patterns produced by their skin. *Biological Bulletin* 193:207-208.

Shashar N, Hanlon RT, Petz AD (1998) Polarization vision helps detect transparent prey. *Nature* 393:222-223.

Shashar, N., Borst, D. T., Ament, S. A., Saidel, W. M., Smolowitz, R. M.and Hanlon, R. T. (2001). Polarization reflecting iridophores in the arms of the squid *Loligo pealeii*. *Biological Bulletin* 201, 267-268.

Stell WK, Lightfoot DO, Wheeler TG, Leeper HF (1975) Goldfish retina: Functional polarization of cone horizontal cell dendrites and synapses. *Science* 190:989-990.

Temple SE (2006) Investigations of Visual Pigment Changes in Fishes. In: Biology. Victoria: University of Victoria.

Temple SE, Plate EM, Ramsden S, Haimberger TJ, Roth W-M, Hawryshyn CW (2006) Seasonal cycle in vitamin A1/A2-based visual pigment composition during the life history of coho salmon (*Oncorhynchus kisutch*). *Journal of Comparative Physiology A* 192:301-313.

Thoreson, W. B. and Burkhardt, D. A. (1990). Effects of synaptic blocking agents on the depolarizing responses of turtle cones evoked by surround illumination. *Visual Neuroscience* 5: 571-583

Thorpe A, Douglas RH, Truscott RJW (1993) Spectral transmission and short-wave absorbing pigments in the fish lens - I. Phylogenetic distribution and identity. *Vision Research* 33:289-300

Tsin AT, Beatty DD (1977) Visual pigment changes in rainbow trout in response to temperature. *Science* 195:1358-1360.

Tsin AT, Leibman PA, Beatty DD, Dryzmala R (1981) Rod and cone visual pigments in the goldfish. *Vision Research* 21:943-946.

Tovee MJ (1995) Ultra-violet photoreceptors in the animal kingdom: their distribution and function. *Trends in Ecology and Evolution* 11:455-460.

Veldhoen K, Allison WT, Veldhoen N, Anholt BR, Helbing CC, Hawryshyn CW (2006) Spatio-temporal characterization of retinal opsin gene expression during thyroid hormone-induced and natural development of rainbow trout. *Visual Neuroscience* 23:169-179.

Ventura, D. F., De Souza, J. M., Devoe, R. D. and Zana, Y. (1999). UV responses in the retina of the turtle. *Visual Neuroscience* 16: 191-204.

Ventura, D. F., Zana, Y., De Souza, J. M. and Devoe, R. D. (2001). Ultraviolet colour opponency in the turtle retina. *Journal of Experimental Biology* 204: 2527-2534.

Verweij J, Kamermans M, Spekreijse H (1996) Horizontal cells feed back to cones by shifting the cone calcium-current activation range. *Vision Research* 36:3943-3953.

Vigh, J. and Witkovsky, P. (1999) Sub-millimolar cobalt selectively inhibits the receptive field surround of retinal neurons. *Visual Neuroscience* 16: 159-168

von Frisch K (1949) Die polarisation des himmelscichtes al orientierender facktor bei den tanzen der bienen. *Experientia* 4:142-148.

Wagner H-J (1990) Retinal Structure of Fishes. In: The Visual System of Fish (Douglas R, Djamgoz M, eds). London: Chapman and Hall.

Wald G, Brown PK (1953) The molar extinction of rhodopsin. *Journal of General Physiology* 37:189-200.

Wang B, Li H, Yan H, Xiao JG (2005) Genistein inhibited hypoxia-inducible factor-1 alpha expression induced by hypoxia and cobalt chloride in human retinal pigment epithelium cells. *Methods and Findings in Experimental and Clinical Pharmacology* 27: 179-184

Waterman TH, Hashimoto H (1974) E-vector discrimination by goldfish optic tectum. *Journal of Comparative Physiology* 95:1-12.

Werblin FS (1974) Control of Retinal Sensitivity .2. Lateral Interactions at Outer Plexiform Layer. *Journal of General Physiology* 63:62-87.

Whitmore AV, Bowmaker JK (1989) Seasonal variation in cone sensitivity and short-wave absorbing visual pigments in the rudd *Scardinius erythrophthalmus*. *Journal of Comparative Physiology A* 166:103-116.

Wietsma JJ, Kamermans M, Spekreijse H (1995) Horizontal cells function normally in ethambutol-treated goldfish. *Vision Research* 35:1667-1674.

Wu, S.M. (1992) Feedback connections and operations of the outer plexiform layer of the retina. *Current Opinion in Neurobiology* 2: 462-478

Yamada M, Low JC, Djamgoz MBA (1992) Chromaticity of synaptic inputs to H1 horizontal cells in carp retina: analysis by voltage clamp and spectral adaptation. *Experimental Brain Research* 89:465-472.

Yazulla S (1995) Neurotransmitter release from horizontal cells. In: Neurobiology and clinical Aspects of the Outer Retina (Djamgoz MBA, Archer SN, Vallerga S, eds), pp 249-271. London: Chapman & Hall.

Young T (1802) On the theory of light and colours. *Transactions of the Royal Society of London* 92:12-48.

Yuan, L.L., and Yang,X.L. (1997) Selective suppression of rod signal transmission by cobalt ions of low levels in carp retina. *Science in China Series C – Life Sciences* 40: 128-136.